

The University of Manitoba

Modal Analysis of Planar Waveguide Junctions

by

C. W. Hasselfield

A Thesis

Submitted to the Faculty of Graduate Studies

in Partial Fulfillment of the Requirements for the Degree

of Master of Science

Department of Electrical Engineering

Winnipeg, Manitoba

1971



ABSTRACT

Planar waveguide discontinuities are studied using the modal analysis method of transverse field matching. The derivation and the methods of calculations are revised from Wexler's method. Several types of junctions with one and two dimensional steps are solved. A new analytic expression is used here to help fit the singularities which may be present in either the electric or magnetic field. A study is made of the uses and limitations of the method in dealing with thin structures, particularly irises.

ACKNOWLEDGEMENT

The author wishes to thank Dr. A. Wexler of the Electrical Engineering Departement, who sugested the topic and guided the research. His interest and encouragement are appreciated.

TABLE OF CONTENTS

ABSTRACT	i
ACKNOWLEDGEMENT	ii
1 INTRODUCTION	1
2 THE MODAL ANALYSIS FORMULATION	4
2.1 Fields at the Junction	4
2.2 Solution of the Forward Scattered Fields and ρ	7
2.3 Back Scattering and the S Matrix	9
3 SOLUTION OF THE H-PLANE STEP	11
3.1 Mode Types Excited	11
3.2 Integral Calculations	13
3.3 Semi-infinite H-Plane Reduction	14
3.4 Transverse Field Plots	17
3.5 Boundary Enlargement	19
3.6 Irises	24

4	SOLUTION OF THE E-PLANE STEP	29
4.1	Mode Types Excited	29
4.2	Integral Calculations	31
4.3	Semi-infinite Symmetrical E-Plane Reduction	32
4.4	Boundary Enlargement	33
4.5	Irises	36
5	TWO DIMENSIONAL STEP	40
5.1	Mode Types Excited	40
5.2	Integral Calculations	43
5.3	Semi-infinite Symmetrical Step	43
5.4	Irises	45
6	FIELD SINGULARITIES	47
6.1	Numerical Treatment of the Singularity	47
6.2	E-Wave on Wedge in Free Space	48
6.3	Special Mode Formulation	50
6.4	Methods of Integrations With Singularities	52
6.5	Modified Solution of the H-plane Step	56
6.6	Modified Solution of the H-plane Bifurcation	57
7	DISCUSSION AND CONCLUSIONS	66
	APPENDIX	68
A.1	Program Description	68
A.2	Modal Equation Derivation	85
	BIBLIOGRAPHY	87

1. INTRODUCTION

Step discontinuities in waveguides have been solved by Wexler (1), Clarricoats and Slinn (2), and Cole, Nagelberg, and Nagel (3) using modal analysis. Among the types of discontinuities that this method is applicable to are semi-infinite E or H-plane steps, rectangular bifurcations of any thickness, thick or thin rectangular irises, irises or steps in circular waveguides, and multiple guide problems.

The method is not without numerical difficulties, particularly in very thin irises and bifurcations. For these problems convergence is a problem and in zero thickness structures the solution does not converge at all. It will be shown here that the field singularities found in steps are dealt with very poorly in the modal analysis solution.

In this work convergence for the H-plane step is investigated and the H-plane iris is studied as a combination of two H-plane steps. The method provides good results for all configurations tested, except for zero thickness structures. An indication of the number of modes required to give a desired accuracy for a given thickness of iris is given here. A solution for the thin iris is attempted as an example of the possible difficulties that arise. Convergence for an iris is found to be

slower as the thickness decreases and in the limit a zero thickness iris was found not to converge at all. A look at the field plots reveals the position and nature of the singularity in the magnetic field. From these plots the attempted field match of the numerical solution is displayed.

The E-plane step is studied next in much the same manner as the H-plane step. Convergence for this problem is found to be similar to the H-plane step but with the method used, twice as many modes are required for the same type of problem. The numerical difficulties of the thin iris are again shown since they are more apparent in this case than they were with the H-plane iris. The two dimensional simultaneous E and H-plane step and iris are investigated next but here a lack of exact solutions makes comparisons difficult. There are however approximate solutions which indicate that the solutions are correct. Convergence to the solution is slower, due to the two dimensional mode types required. Only approximate results can be obtained without setting up very large systems of linear equations.

Difficulties due to the singularity are partially resolved by using a combination of the analytic solution near the edge and the normal waveguide modes on the H-plane step. It is found that faster convergence and better field matching is obtained with this combination method. The number of calculations is increased however since the analytic solution must be made orthogonal to the normal waveguide modes for the modal analysis method to be

3.

applied.

A new notation simpler than Wexler's is presented here with an alteration allowing any mode incident, not just the dominant first one.

2. THE MODAL ANALYSIS FORMULATION

Any discontinuity problem in a reciprocal waveguide, that has a series of planar junctions such as an iris, can be solved by modal analysis. Each junction is treated separately, taking into account scattering from neighboring junctions. The fields on either side of the junction are expressed as a series of normal waveguide modes and these fields are equated across the junction. The technique for solving for the unknown series coefficients is given here and the expression for the interaction of the planar junctions is presented.

2.1 Fields at the Junction

Top and end views of a representative junction problem are given in Fig. 2.1. An incident mode, numbered r with coefficient a_r , impinges upon junction m in the z direction. Let the waveguide section on the generator side of junction m be denoted $A_{(m)}$ and the waveguide section on the load side be denoted $B_{(m)}$. Using this notation on a multiguide section, the dimensions of section $A_{(m+1)}$ equal section $B_{(m)}$. The fields at junction m , on the generator side are expanded in terms of the normal waveguide

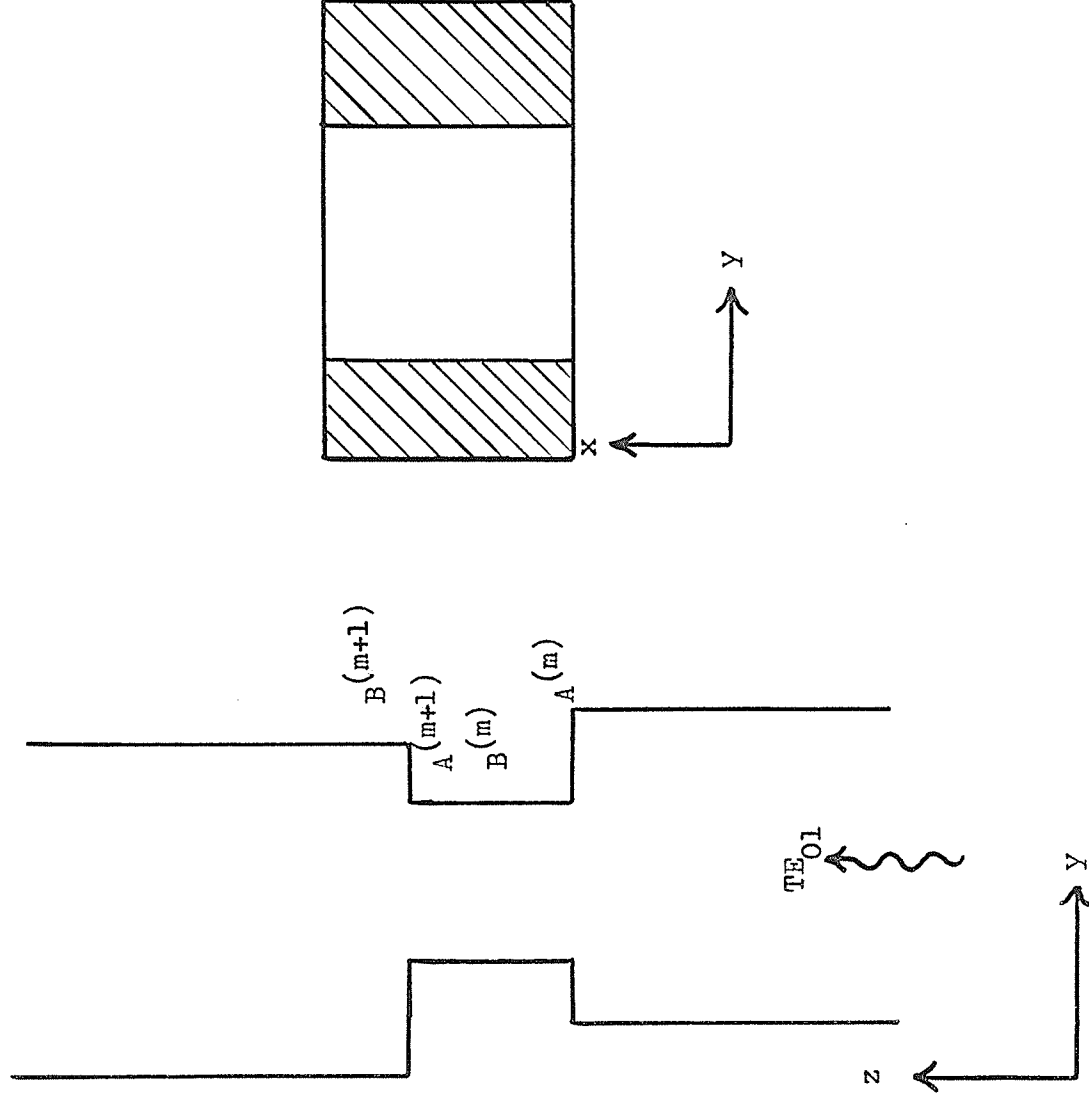


Fig. 2.1 Top and end view of a discontinuity in a waveguide

modes in $A^{(m)}$ and are given by Wexler(4) as

$$\overline{E} = (1 + \rho_r) a_r \overline{e}_{ar} + \sum_{\substack{i=1 \\ i \neq r}}^{\infty} a_i \overline{e}_{ai} \quad (2.1)$$

and

$$\overline{H} = (1 - \rho_r) a_r \overline{h}_{ar} + \sum_{\substack{i=1 \\ i \neq r}}^{\infty} a_i \overline{h}_{ai} \quad (2.2)$$

The transverse vector mode functions \overline{e}_{ak} and \overline{h}_{ak} for guide $A^{(m)}$ are known in advance. The corresponding mode coefficients for the functions are a_r and ρ_r and the total transverse electric and magnetic fields are \overline{E} and \overline{H} . If γ_i is the z-dependent propagation constant of the i-th mode in $A^{(m)}$, then any mode may be referred a distance λ towards the source by multiplying by $e^{\gamma_i \lambda}$.

The same field may be expressed on the load side of junction m by a series of modes of waveguide section $B^{(m)}$ as follows:

$$\overline{E} = \sum_{j=1}^{\infty} b_j \overline{(e_{bj})} + \sum_{k=1}^{\infty} s_{jk} \overline{e_{bk}} \quad (2.3)$$

and

$$\overline{H} = \sum_{j=1}^{\infty} b_j \overline{(h_{bj})} - \sum_{k=1}^{\infty} s_{jk} \overline{h_{bk}} \quad (2.4)$$

The scattering coefficients s_{jk} of (2.3) and (2.4) account for the contribution from the j -th mode incident on junction $m+1$ from junction m and scattered back to junction m as the k -th mode. This scattering matrix S , contains information about the propagation of the modes involved between junctions m and $m+1$, and also the scattering properties of junction $m+1$.

For this reason the last junction nearest the load must be solved first, with the assumption that it is followed by a simple or known termination, such as a short or a matched load. Any junction numbered m falls into two general classes: boundary reduction where section $A^{(m)}$ is larger than section $B^{(m)}$; and boundary enlargement where section $A^{(m)}$ is smaller than section $B^{(m)}$.

2.2 Solution of the Forward Scattered Field and ρ

For the solution of junction m , the scattering matrix S , due to the cumulative effect of junctions in the direction of the load, is known. The derivation given by Wexler (4), generalized to allow the r -th mode incident on a junction, rather than only the first mode, is shown in appendix A.2. The results are

$$\rho_r \delta_{nr} + \sigma \sum_{j=1}^N \left[\frac{b_j}{a_r} \sum_{i=1}^M \delta_{ji} + \sigma \frac{\sum_{k=1}^N s_{jk} \delta_{ki} \delta_{ni}}{\alpha_i} \right] \beta_n = \sigma \delta_{nr} + \sigma \left(\frac{b_m}{a_r} - \sigma \sum_{j=1}^N \frac{b_j}{a_r} s_{jn} \right) \beta_n = \sigma \delta_{nr} \quad (2.5)$$

$n = 1, 2, 3, \dots, N$

and

$$\rho_r \alpha_r - \sigma \sum_{j=1}^N \frac{b_j}{a_r} (\delta_{jr} + \sigma \sum_{k=1}^N s_{jk} \delta_{kr}) = -\sigma \alpha_r \quad (2.6)$$

where

$$\delta_{ij} = \int_b \overline{e_{bj}} \times \overline{h_{ai}} \cdot \tilde{u}_z \, ds \quad (2.7)$$

$$\alpha_i = \int_a \overline{e_{ai}} \times \overline{h_{ai}} \cdot \tilde{u}_z \, ds \quad (2.8)$$

$$\beta_j = \int_b \overline{e_{bj}} \times \overline{h_{ai}} \cdot \tilde{u}_z \, ds \quad (2.9)$$

and

$$\sigma = 1 \quad (2.10)$$

For the boundary enlargement problem, (2.7) and (2.10) are replaced by

$$\delta_{ij} = \int_a \overline{e_{ai}} \times \overline{h_{bj}} \cdot \tilde{u}_z \, ds \quad (2.11)$$

and

$$\sigma = -1 \quad (2.12)$$

The series in (2.5) and (2.6) have been truncated to M and N modes in guide $A^{(m)}$ and $B^{(m)}$ respectively. Since (2.5) supplies N linear complex equations and (2.6) supplies one more, the set can be solved yielding the coefficients $\rho_r, \frac{b_1}{a_r}, \frac{b_2}{a_r}, \dots, \frac{b_N}{a_r}$.

2.3 Back Scattering and the S Matrix

Using the solved coefficients, the back scattered mode coefficients $\frac{a_i}{a_r}$ are computed by

$$\frac{a_i}{a_r} = \frac{\sigma \sum_{j=1}^N \frac{b_j}{a_r} (\delta_{ji} + \sum_{k=1}^N s_{jk} \delta_{ki})}{\alpha_i} \quad (2.13)$$

which completes the analysis of junction m.

The scattering matrix S for the next junction, numbered m-1, at a distance ℓ towards the source, can now be assembled. For each mode r incident on junction m, there are M scattering coefficients for junction m-1 which are given by

$$S_{ri} = \begin{cases} \frac{a_i}{a_r} e^{-(\gamma_i + \gamma_r)\ell} & i \neq r \\ \rho_r e^{-2\gamma_r \ell} & i = r \end{cases} \quad \begin{matrix} i = 1, 2, \dots, M \\ i = r \end{matrix} \quad (2.14)$$

where the a_i are for junction m. There is a term of the form (2.14) for each of the M modes incident on junction m, thus generating M^2 scattering coefficients.

When power enters a system of connected waveguides with discontinuities, the incident modes are scattered at junction 1 and propagated, according to the waveguide dimensions, to

junction 2 as an infinite number of forward scattered modes. At junction 2 this infinite set of modes are again scattered individually, some propagating back to junction 1 and others propagating to junction 3. In this way the properties of a junction are dependent on the junctions further down the guide.

3 SOLUTION OF THE H-PLANE STEP

Approximations for various H-plane step configurations with known accuracy limits are given by Marcuvitz (5) for ranges of frequency and step width.

The types of modes excited and the calculation using them are given here for the H-plane step. Integrations involving them are done numerically rather than by using analytic results. The solution of the step is given and the transverse field plots show the degree of field match. The corresponding boundary enlargement problem is studied in order that the H-plane iris can be solved.

3.1 Mode Types Excited

For an incident TE_{0i} mode on the simple junction of Fig. 3.1, the only type of mode which can be excited are of the TE_{0N} type. If the discontinuity is symmetrical about an x direction symmetry line, then if i is odd, N is odd and if i is even, N is even.

Assuming TE_{01} incident the expression for the transverse E

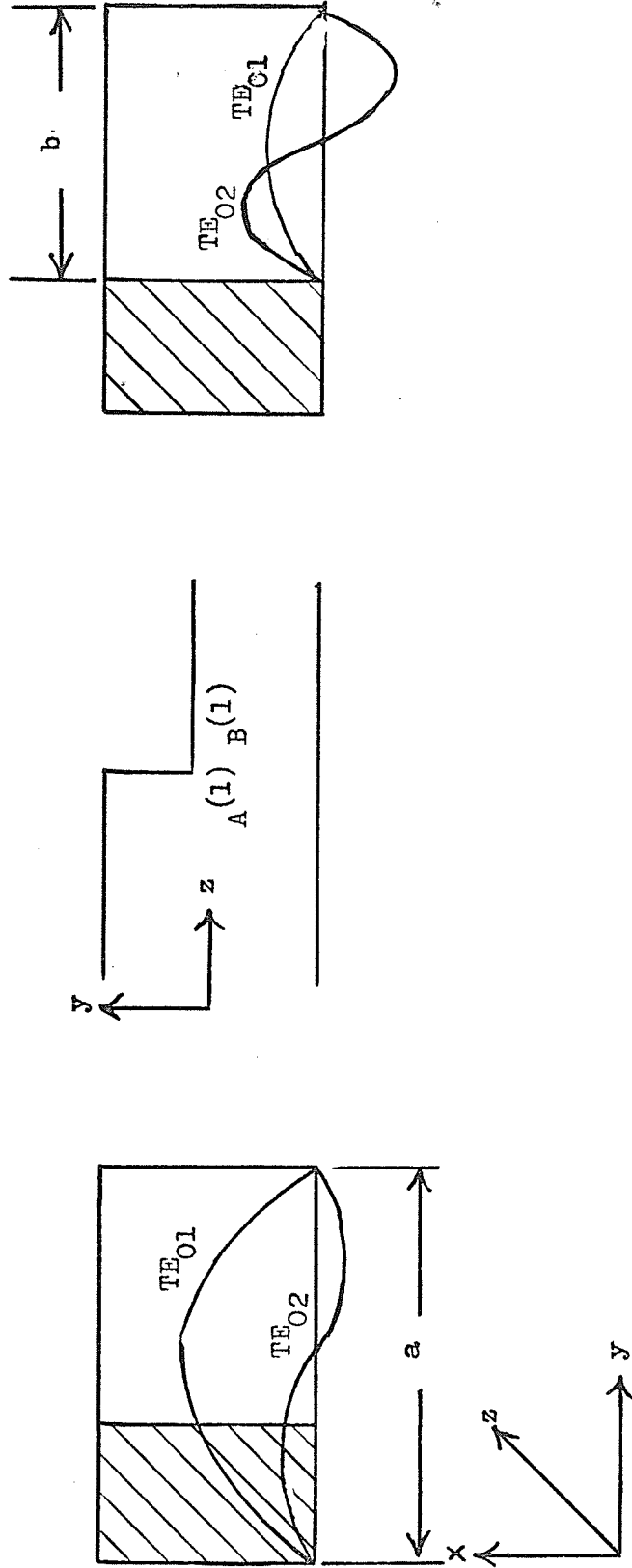


Fig. 3.1 End and top views of junction showing magnitude of electric field on opposite sides of a junction

and H fields for the i-th mode in guide A⁽¹⁾ are

$$\bar{e}_{ai} = \frac{j\omega\mu}{k_{ci}^2} k_{yi} \sin k_{yi} y \bar{u}_x \quad (3.1)$$

$$\bar{h}_{ai} = \frac{\gamma_i}{k_{ci}^2} k_{yi} \sin k_{yi} y \bar{u}_y \quad (3.2)$$

where

$$k_{yi} = \frac{i\pi}{a} \quad (3.3)$$

$$\gamma_i^2 = k_{yi}^2 - \omega^2 \mu \epsilon \quad (3.4)$$

and

$$k_{ci}^2 = k_{yi}^2 \quad (3.5)$$

and the frequency ω is in radians/sec.

Similar expressions hold for the i-th mode of B⁽¹⁾ but here

$$k_{yi} = \frac{i\pi}{b} \quad (3.6)$$

3.2 Integral Calculations

The integrals of (2.7-2.9) and (2.11) are calculated numerically rather than analytically as done by Wexler (5). Even though analytic expressions for α_i and β_i could be obtained for the two dimensional steps discussed later, a general expression for δ_{ij} would be practically impossible for these configurations.

The integration routine used was a modified version of the

IBM scientific subroutine package program QATR which uses mesh halving with Simpson's trapezoidal rule and Richardson's extrapolation using two successive steps. By calculating the difference between each step a measure of the accuracy can be obtained. The integrands of (2.7) and (2.11) behaved in such a way that the rounding error did not decrease monotonically for every mesh halving. All calculations were done in single precision. For this reason checks had to be built in to be sure that rounding error was indeed larger than discretization error. In all test cases the integration results came to within five significant figures of the exact answer for all mode types used. For the higher order modes used, the discretization error became more of a problem and hence more mesh halving was necessary and thus rounding error limited the accuracy of the results. For the maximum mode order used here, ie. 30, no accuracy problems were encountered.

3.3 Semi-Infinite H-Plane Reduction

As a test case for the program, the step in Fig. 3.2 was studied. With an incident TE_{01} mode, the mode types excited are TE_{0n} with $n = 1, 3, 5, \dots$. All calculations are done using standard X-band guides, with no loss of generality, as all examples can be scaled.

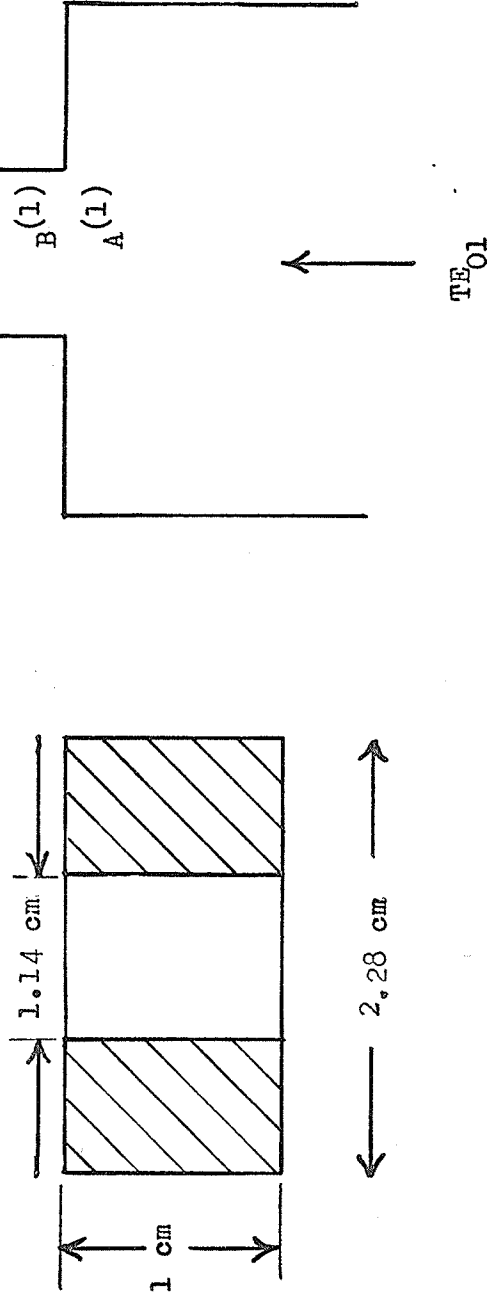


Fig. 3.2 H-plane step. End and top view

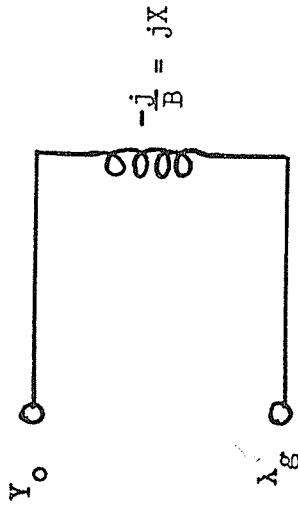


Fig. 3.3 Equivalent circuit of H-plane step of Fig. 3.2
 Y_0 is guide admittance and λ_g is guide wavelength

f (GHz)	From Modal Analysis		
	Marcuvitz	M=N=10	M=N=15
8	-4.46	-4.430	-4.441
9	-3.13	-3.093	-3.101
10	-2.28	-2.323	-2.330
11	-1.77	-1.788	-1.773
12	-1.17	-1.292	-1.290

Table 3.1 Equivalent circuit for H-plane step. TE_{03} mode propagate at 19.65 GHz. and cutoff for TE_{01} mode in section B(1) is 13.1 GHz.

Convergence for this type of junction was quite rapid and the error due to the number of modes used decreased with increasing M and N . For $M = N = 3, 10,$ and 15 the calculated normalized impedance of the equivalent circuit of Fig. 3.3 given by Marcuvitz (7) are compared in Table 3.1. Marcuvitz estimates the error to be less than 1%. The small real part of the admittance is due to the rounding error of the equation solution and should in theory be exactly zero, that is, it has a reactive load even for finite M and N , since the guide is lossless and is in cutoff after the junction.

3.4 Transverse Field Plots

The total field expressions of (2.1) to (2.4) can be used to produce plots of the E and H fields on the generator and load side of the junction. For a frequency of 10 GHz, the E and H magnitudes are shown in Fig. 3.4 for the three modal series truncations.

The E and H fields in guide $B^{(1)}$ are defined to be zero from the equation to the left of the conductor wall at $y = 0.5715$ cm. and in both guides the fields are symmetric about the center line at $y = 1.143$ cm.

The E field shows a progressively better match within the guide as the number of modes increases. The H field however is

18.

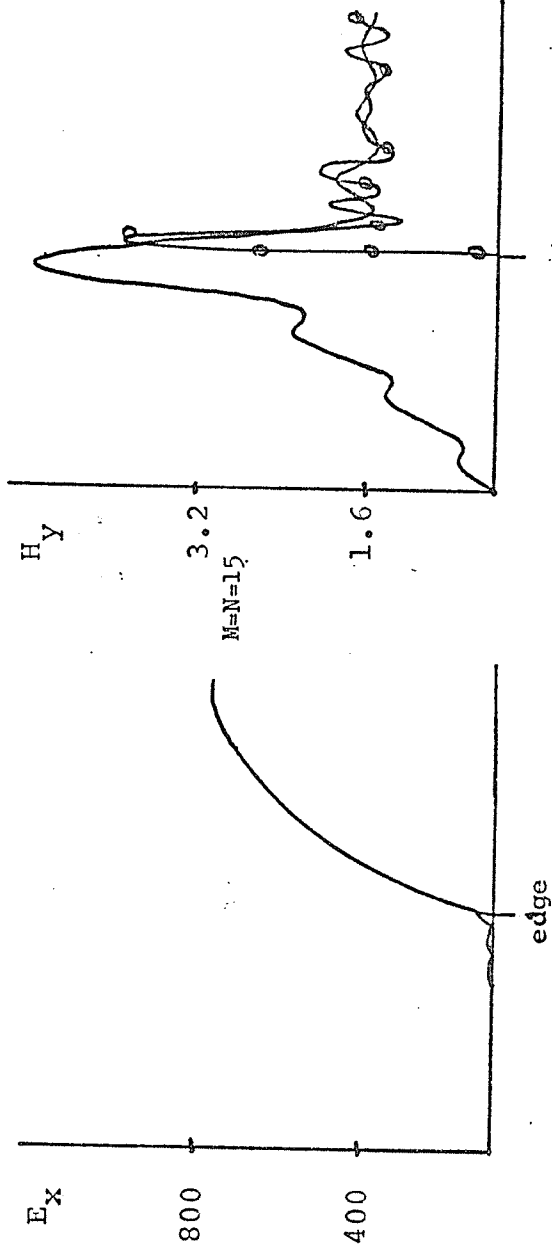
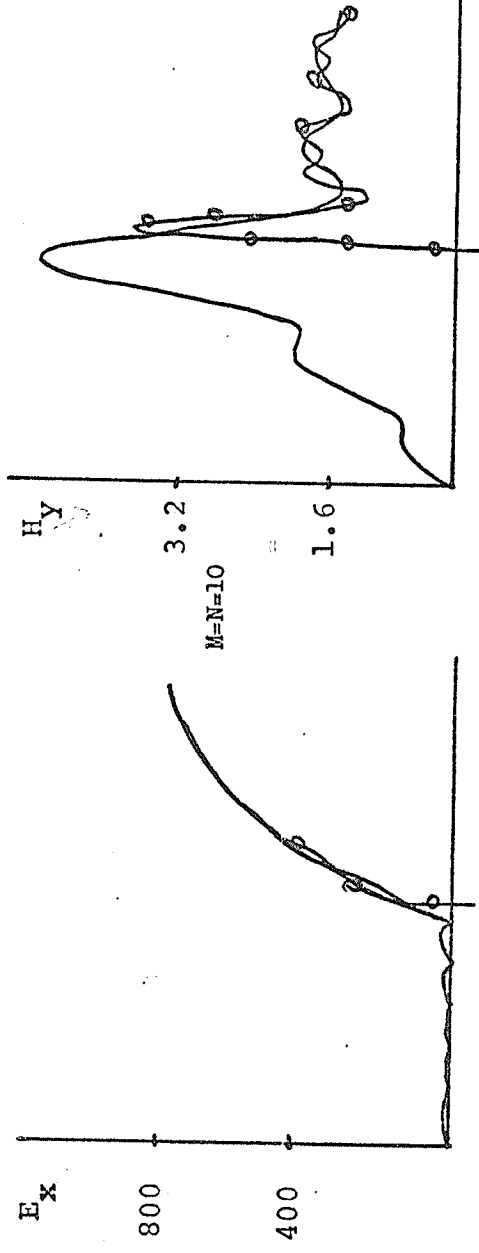
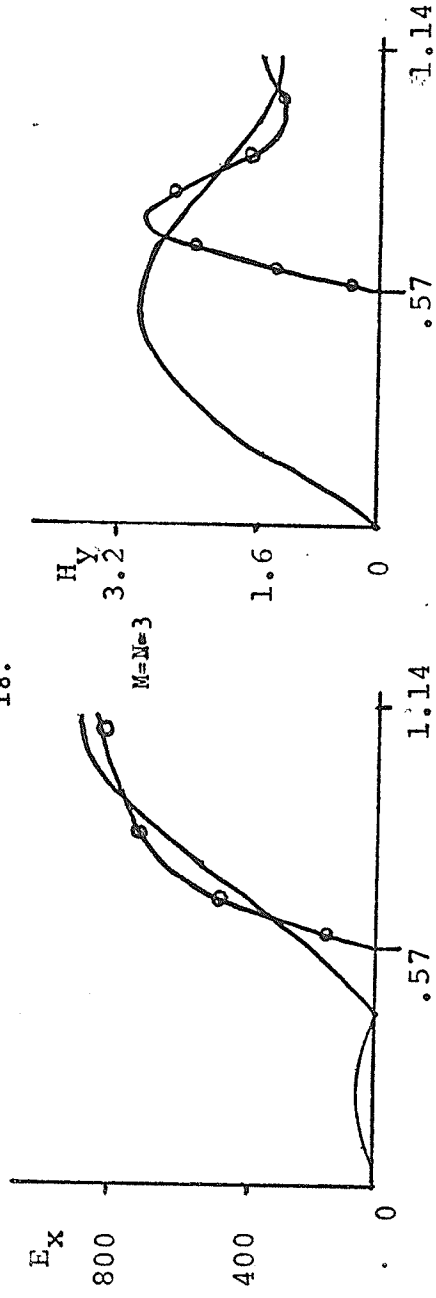


Fig. 3.4 Magnitudes of field match electric fields on right magnetic on left. Solid curve field in section A, circled curve section B

not as good a match. There is a singularity at the metal edge, the field going to infinity. It can be seen that the H field in guide $A^{(1)}$ rises on the face of the edge while in guide $B^{(1)}$ the field rises inside the guide. As the number of modes increases the peaks become higher and closer to the edge. The H field in $B^{(1)}$ has particular trouble since the mode functions that make up the total are each zero at the edge but the sum at the edge should be infinite in the limit. Note that the H field in $A^{(1)}$ on the face of the edge is not zero as is the E field.

3.5 Boundary Enlargement

As a prelude to solving the thick iris, the semi-infinite H-plane enlargement of Fig 3.5 was studied. Guide $A^{(1)}$ was excited by a TE_{01} mode at a frequency of 16 GHz., so that it was not in cutoff. The resulting normalized input admittance for a matched termination on $B^{(1)}$ and $M = N = 10$ was

$$Y = 1.1810 - j0.3999 \quad (3.7)$$

Here the real part results from power flowing down guide $B^{(1)}$ and has unit magnitude with respect to the characteristic guide admittance in $B^{(1)}$. The equivalent circuit, shown in Fig. 3.6, omits the shift of reference plane for guide $B^{(1)}$ since it is

0.002 cm towards the generator as calculated by Marcuvitz (8) and is negligible.

A check of the solution can be obtained by finding the input admittance of the same junction excited from the opposite side and terminated in a matched load. The configuration is shown in Fig. 3.2 but the frequency was kept at 16 GHz., since cutoff for this section is at 13.1 GHz. The normalized input admittance using $M = N = 10$ for this reduction problem was

$$Y = 0.8381 - j.03325 \quad (3.8)$$

This circuit is shown in Fig. 3.7. The real part of (3.8) is the matched load seen by the junction and is thus $\frac{Y'_O}{Y_O}$ for the reduction. The real part in (3.7) is again the load on the junction and is $\frac{Y'_O}{Y_O}$ for a boundary enlargement. Since the real part of (3.7) and (3.8) are not quite inverses, an indication of the error can be obtained. The reduction admittance ratio $\frac{Y'_O}{Y_O}$ which is the real part of (3.7) can be checked by an expression from Marcuvitz (9). The impedance ratio is given as

$$\frac{Z'_O}{Z_O} = \frac{Y_O}{Y'_O} = 1.2 \quad (3.9)$$

The inverse of this is 0.834 and the limit of error is given as 10%. This inverse however compares favorably with the real part of (3.8) as does the ratio in (3.9) compare with the real part of (3.7). Thus the imaginary part divided by the real part in (3.7)

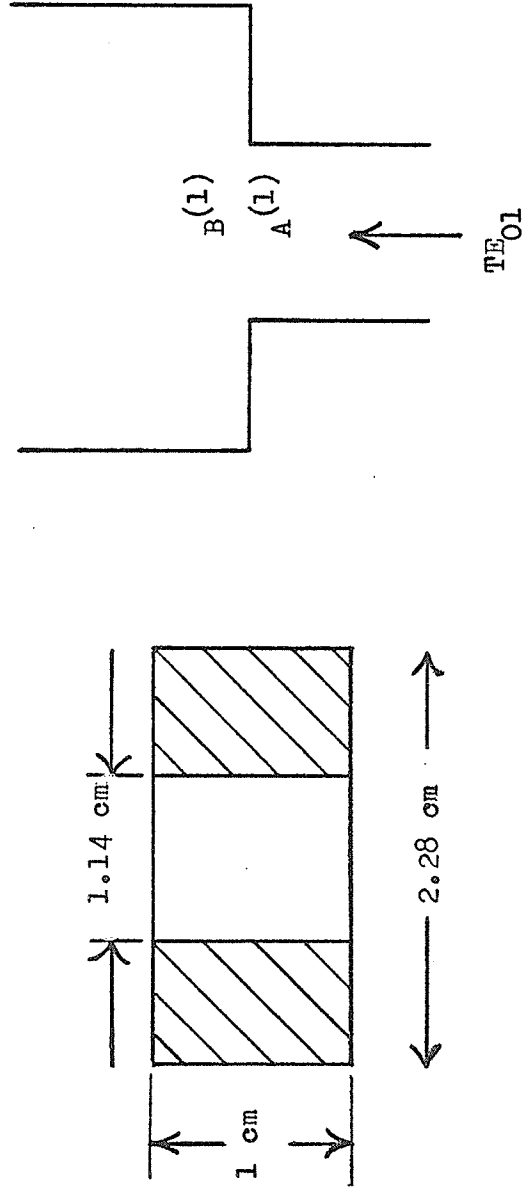


Fig. 3.5 H-plane step end and top views

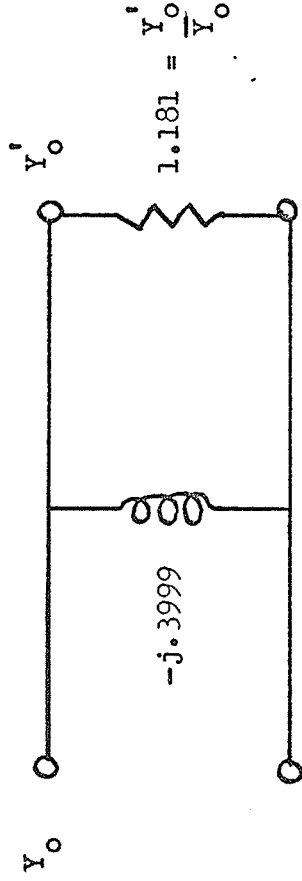


Fig. 3.6 Equivalent circuit of H-plane step showing normalized admittance with respect to guide A. The admittance in B is Y'_0 .

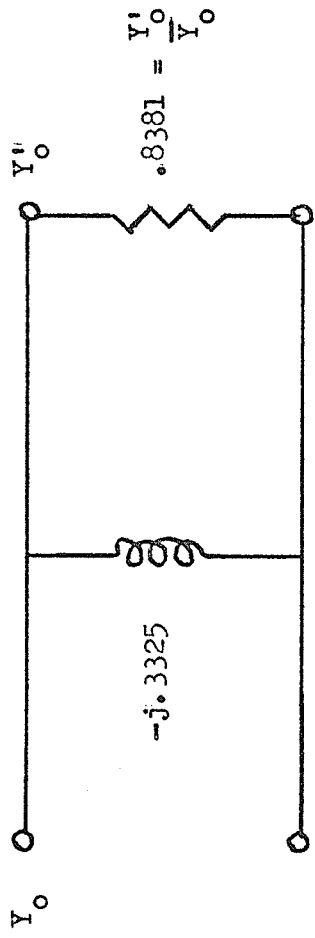


Fig. 3.7 Equivalent circuit of H-plane step $f = 16$ GHz.

gives the imaginary part of (3.8) and vice versa since (3.7) can be written as

$$Y = \frac{Y'_O}{Y_O} - j \frac{B}{Y_O}$$

and

$$\frac{\frac{B}{Y_O}}{\frac{Y'_O}{Y_O} - j \frac{B}{Y_O}} = \frac{B}{Y'_O} \quad (3.10)$$

The configuration of Fig. 3.5 was tested for $f = 10$ GHz with the wave impinging on the discontinuity in cutoff. The normalized input admittance was

$$Y = 0.5786 + j0.6655 \quad (3.11)$$

There are no available results to compare with. Here the normalized admittance Y_O is a negative imaginary number and the characteristic impedance ratio is

$$\frac{Y'_O}{Y_O} = j \cdot 0.6655 \quad (3.12)$$

with Y'_O real. The real part of the admittance represents an inductance which can be seen if it is normalized with respect to guide $B^{(1)}$.

$$\frac{B}{Y_O} = \frac{.5715}{\frac{Y'_O}{Y_O}} = \frac{0.5786}{j \cdot 0.6655} = -j \cdot 867 \quad (3.13)$$

The enlargement studied here will be used next in the study of irises.

3.6 Irises

The thick symmetrical iris of Fig. 3.8 was studied by considering it to be two coupled discontinuities of the type of Sections 3.3 and 3.5. A π equivalent circuit of the iris at the reference planes T, as given by Marcuvitz (10), is shown in Fig. 3.9. Note that Y_{12} is defined to be positive here. Due to the symmetry of the iris there are only two parameters to be determined for the equivalent circuit. Since the circuit is lossless, an open and a short circuit at the load plane T will completely determine Y_{11} and Y_{12} .

For a given load, the discontinuity at the load side is solved first and with $M = N = 10$ the back scattering coefficients for the ten lowest modes incident on the junction are found. Then these are transformed through the distance l and the load side discontinuity with an incident TE_{01} mode is solved.

For the first junction, the s_{jk} terms are set to correspond to the type of load required. For a short circuit at the load side T

$$s_{jj} = - e^{-(\lambda g/2)} (2 \gamma_j)$$

and

$$s_{jk} = 0 \quad , \quad j \neq k \quad (3.14)$$

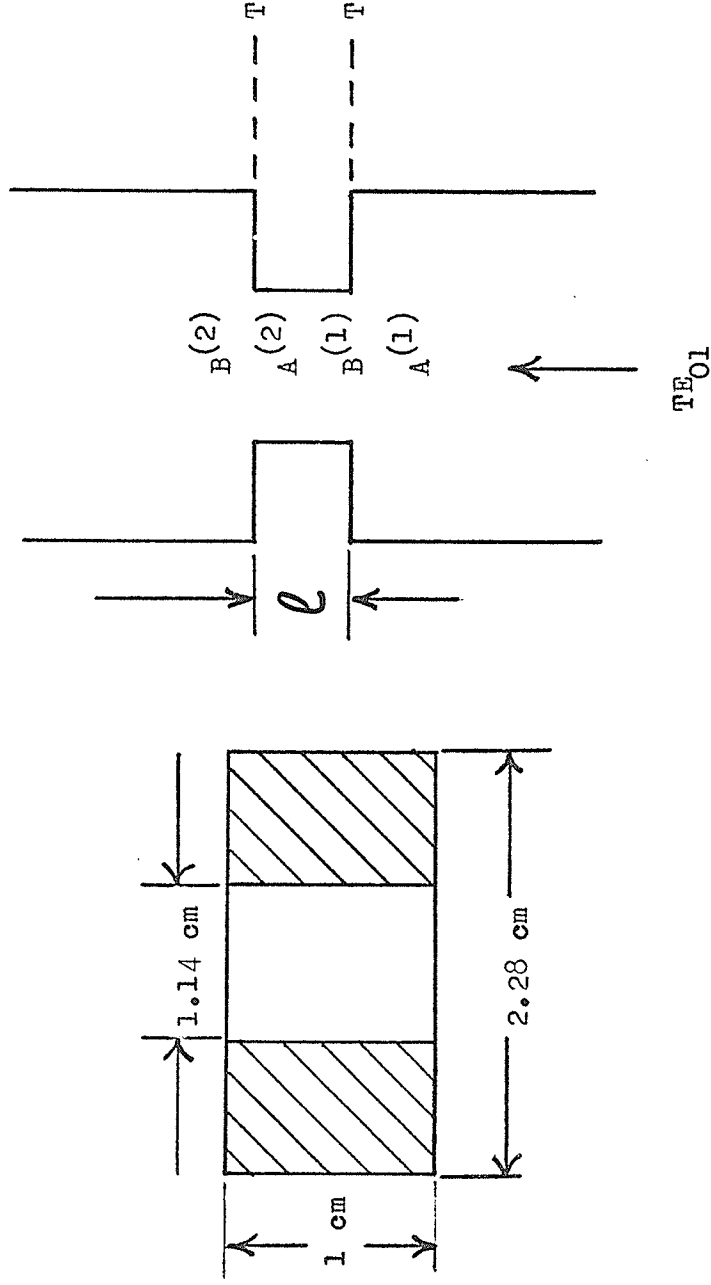


Fig. 3.8 Symmetrical iris, end and top view

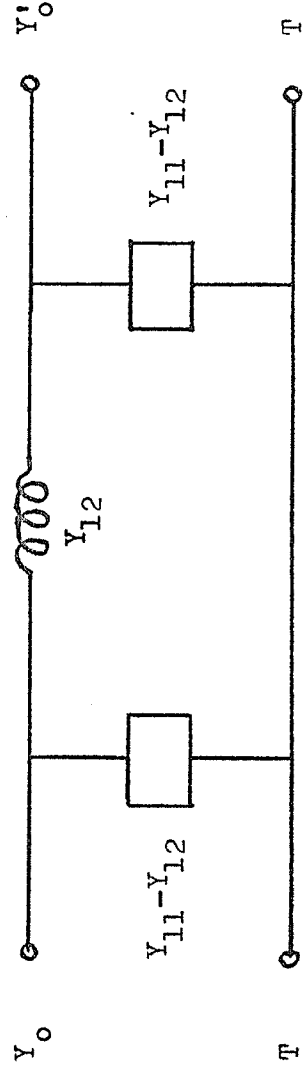


Fig. 3.9 Equivalent circuit of thick iris of Fig. 3.8

and for an open circuit

$$s_{jj} = - e^{-(\lambda g/4)} (2 Y_j)$$

and

$$s_{jk} = 0, \quad j \neq k \quad (3.15)$$

Approximate results are given by Marcuvitz (11) but no maximum limit is set on the error. For $\ell = 2$ cm. and $f = 10$ GHz, the value given for Y_{11} , Y_{12} and Y_{12} are $j0.434$ and $-j0.594$ respectively. The resulting values from modal analysis are $j0.401$ and $-j0.560$.

In order to approximate a zero thickness iris the thickness ℓ is set small but not exactly zero. The difficulty is that the slow convergence for thin vanes, as pointed out by Wexler (12), apply here also and so the thickness of the iris was reduced until numerical problems arose. Then tests were run on the thinnest case that gave no numerical problems.

It was found that an iris with thickness 0.03 cm. gave an equivalent circuit of Fig. 3.10 with negligibly small upper arms values, while still giving good convergence in modal analysis. A thickness of half that did not converge. Note that the reference planes are at T , not at the center of the iris as in Marcuvitz (13), so that the upper arms are thus inductive rather than capacitive. Table 3.2 gives a comparison of the thin iris circuit values for $f = 10$ GHz and $\ell = 0.03$ cm. The upper-arm values have converged to $j0.019$ and Z_{12} is converging to a value that is within 10% of the zero thickness iris. Any attempt to

converging to a value that is within 10% of the zero thickness iris. Any attempt to decrease the thickness resulted in more and more modes required for convergence.

An extension of the modal analysis method is presented by Masterman, Clarricoats and Hannaford (15) for the solution of zero thickness irises. It involves writing one set of field functions in the iris that must match the normal waveguide modes just outside the iris. They use normal waveguide mode functions but with no impedance defined between the E and H fields, that is, separate series for the electric and magnetic fields. Their results are accurate for only one ratio of functions in the aperture, to functions outside the aperture. The value of this ratio must be determined experimentally and an empirical rule is given to approximate this ratio. The justification for this method is that the separate series for the magnetic field allows it to independently approximate the field. The expressions for the fields outside the aperture are not independent and thus can give no better approximation. The success of the method may be due to the optimum M/N ratio rather than the aperture functions. It is noted that the aperture functions are already orthogonal to each other, thus making the method simpler than in Chapter six.

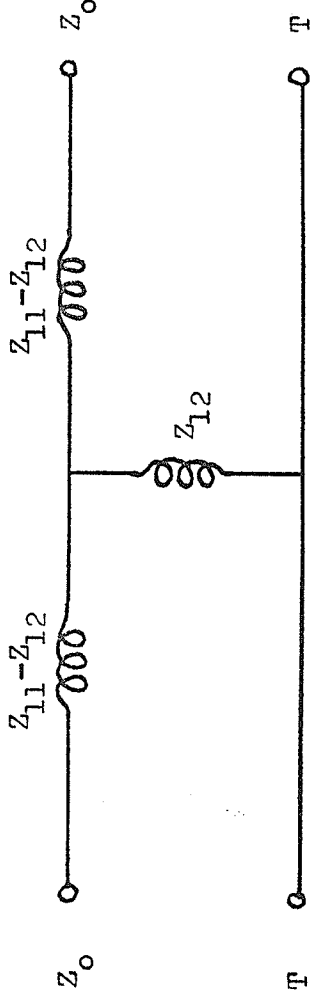


Fig. 3.10 Equivalent circuit of thin iris of Fig. 3.3

Iris of	$Z_{11} - Z_{12}$	Z_{12}
zero thickness Marcuvitz	0	j.637
Modal	M=N=8	j.615
	M=N=10	j.603
	M=N=12	j.596

Table 3.2 Equivalent circuit parameter values of Fig. 3.10
Thickness was .03 cm. Values are normalized to
the guide admittance.

4 SOLUTION OF THE E-PLANE STEP

As a parallel to the study of the H-plane step, the E-plane step is investigated with similar configurations as laid out in the previous chapter. An exact expression for the impedance is available for the change of height which gives another independent check of the results. Limitations are indicated for the degree of accuracy for steps and irises.

4.1 Mode Types Excited

The change of height, or semi-infinite E-plane step, is shown with the co-ordinate system given in Fig. 4.1. If there is an incident TE_{01} mode in guide $A^{(1)}$, then because of the symmetry in the y direction, the mode types excited are transverse electric to x, TE_{xm1} , or LSE_{m1} modes. If the discontinuity is symmetrical about a center line in the y direction, then m is even only. These TE_{xm1} modes can also be expressed as the sum of TE_{m1} and TM_{m1} modes for each m. To keep the program general the ordinary TE_{m1} and TM_{m1} modes are used rather than using the TE_x modes.

The transverse E and H field functions for a TE_{m1} and TM_{m1}

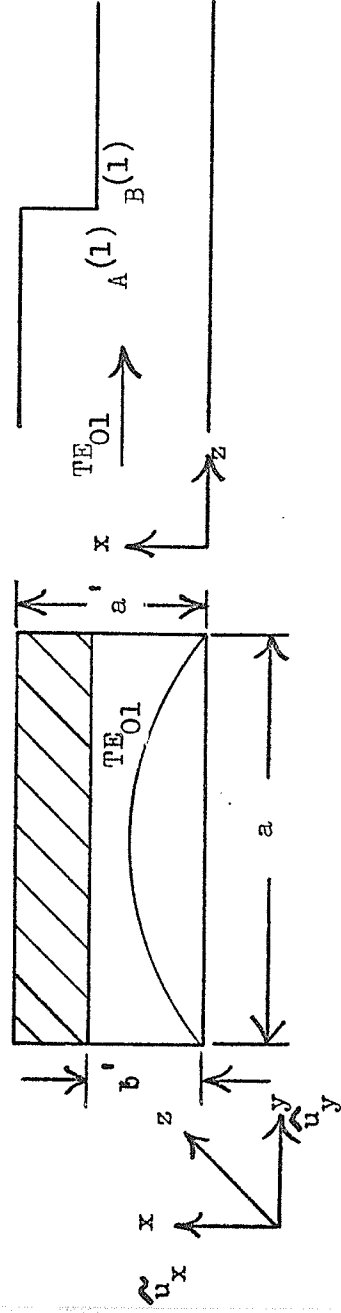


Fig. 4.1 E-plane step with incident TE_{01} mode

mode are then the following:

TE_{m1} modes

$$\bar{e}_{ai} = \frac{j\omega\mu}{k_{cm1}^2} (k_{y1} \cos k_{xm} \text{xsink}_{y1} \text{y}\ddot{u}_x - k_{ym} \text{sink}_{xm} \text{xcosk}_{y1} \text{y}\ddot{u}_y) \quad (4.1)$$

$$\bar{h}_{aj} = \frac{\gamma_{m1}}{k_{cm1}^2} (-k_{xm} \text{sink}_{xm} \text{xcosk}_{y1} \text{y}\ddot{u}_x - k_{y1} \cos k_{xm} \text{xsink}_{y1} \text{y}\ddot{u}_y) \quad (4.2)$$

and TM_{m1} modes

$$\bar{e}_{aj} = \frac{\gamma_{m1}}{k_{cm1}^2} (k_{xm} \cos k_{xm} \text{xsink}_{y1} \text{y}\ddot{u}_x - k_{y1} \text{sink}_{xm} \text{xcosk}_{y1} \text{y}\ddot{u}_y) \quad (4.3)$$

$$\bar{h}_{aj} = \frac{j\omega\epsilon}{k_{cm1}^2} (k_{y1} \text{sink}_{xm} \text{xcosk}_{y1} \text{y}\ddot{u}_x - k_{xm} \cos k_{xm} \text{xsink}_{y1} \text{y}\ddot{u}_y) \quad (4.4)$$

where

$$k_{xm} = \frac{m\pi}{a} \quad k_{y1} = \frac{\pi}{a}$$

$$\gamma_{m1}^2 = k_{xm}^2 + k_{y1}^2 - \omega^2\mu\epsilon \quad (4.5)$$

$$k_{cm1}^2 = k_{xm}^2 + k_{y1}^2$$

Similar modes are excited in guide B⁽¹⁾ but with

$$k_{xm} = \frac{m\pi}{b} \quad (4.6)$$

In guide B⁽¹⁾ there is also a TE₀₁ mode.

4.2 Integral Calculations

Since the modes are two dimensional functions, a two

dimensional integration is now required. However the modes described in (4.1-4.4) are always products of x and y functions, and thus the double integration can be broken into the sum of the product of two one-dimensional integrations. The result is that the number of function evaluations is proportional to the sum of the grid evaluations in each co-ordinate direction rather than the product. This simplification can be used in most rectangular and circular problems. The integrations are then calculated as described in Sec. 3.2 since now the functions involved are exactly the same.

4.3 Semi-infinite Symmetrical E-plane Reduction

Modal analysis was applied to the E-plane step of Fig. 4.2 to obtain the reflection coefficient of the TE_{01} incident mode. The mode types excited here are TE_{m1} and TM_{m1} ($m = 2, 4, 6, \dots$) in guide $A^{(1)}$ and TE_{01} plus TE_{m1} and TM_{m1} ($m = 2, 4, 6, \dots$) in guide $B^{(1)}$.

Convergence for this step was not as rapid as with the H-plane step. In addition there are twice as many modes required to get the same mode order since both TE and TM modes are used. In spite of this the equivalent circuit obtained, using only the ten lowest order modes, agrees well with standard references.

The circuit of Fig. 4.3 has a capacitive value within 3% of Marcuvitz (16) which is within the error limit given in the reference for $f = 10$ GHz.

The characteristic impedance ratio is given by the exact expression

$$\frac{Y'_O}{Y_O} = \frac{b}{b'} \quad (4.7)$$

The conductance for the matched load case, of Fig. 4.2, is 1.5 mhos which is exactly the value of the impedance ratio

$$\frac{b}{b'} = 1.5 \quad (4.8)$$

This indicates that the real part has converged faster than the imaginary part.

4.4 Boundary Enlargement

As in Chapter 3, the boundary enlargement problem must be solved before most multi-junction problems are handled. The step of Fig. 4.4 was solved using the ten lowest modes again. The resulting equivalent circuit with the load corresponding to a matched load is shown in Fig. 4.5.

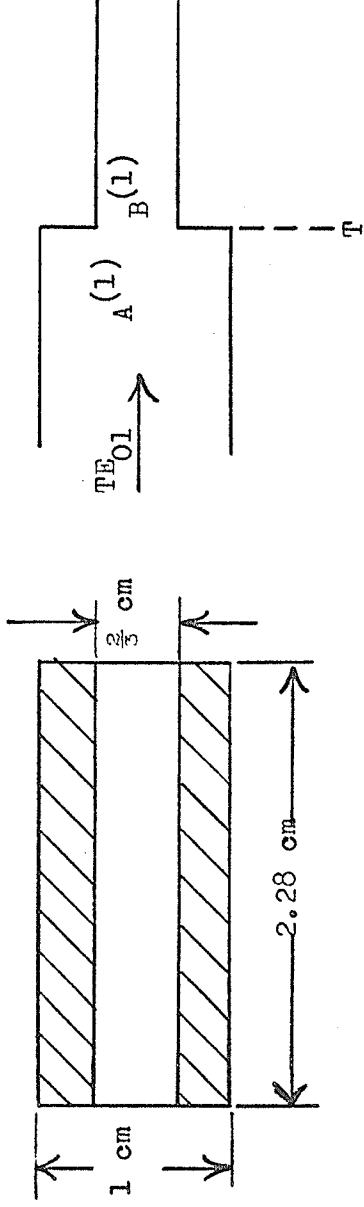


Fig. 4.2 Symmetrical E-plane step. End and side view of reduction

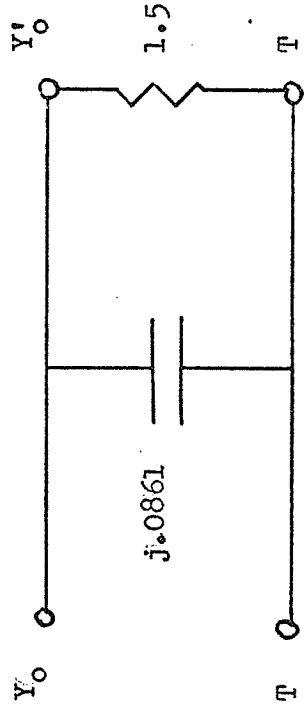


Fig. 4.3 Equivalent circuit of E-plane step with load

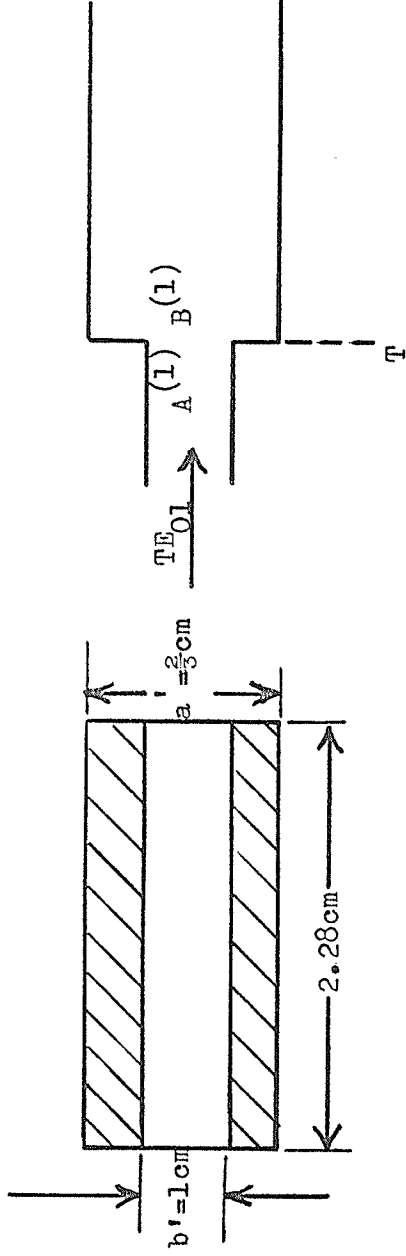


Fig. 4.4 E-plane step enlargement. End and side view

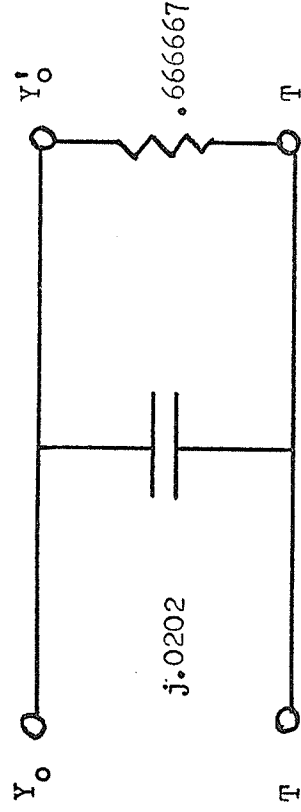


Fig. 4.5 Equivalent circuit of E-plane enlargement with matched load

4.5 Irises

The symmetrical iris shown in Fig. 4.6 is studied as in Section 3.6 where it is considered as two coupled simple discontinuities. The equivalent circuit is given in Fig. 4.7. Due to the symmetry of the iris about a transverse plane, there are again only two parameters to be determined, Y_{12} and $Y_{11} - Y_{12}$. An open and short circuit termination are placed at the load reference plane T and the reflection coefficient of the unit incident TE_{01} mode is found for each case. The s_{jk} terms are determined as in (3.13) and (3.14).

For $M = N = 12$ the equivalent circuit obtained is compared to the circuit from Marcuvitz (17) in Fig. 4.8. The difference in circuit values is well within the upper limit of error as stated by Marcuvitz.

In an attempt to approximate the zero thickness iris, the T equivalent circuit is found rather than the π for comparison purposes. In this case convergence is more of a problem than with the inductive iris. The circuit values for $M = N = 16$ are obtained. The circuit given by Marcuvitz (18) is shown with the circuit obtained by modal analysis for $\lambda = 0.03$ cm. in Fig. 4.9. The values of the upper arms are calculated by modal analysis to be zero so are not shown. The lower arm member agrees to within

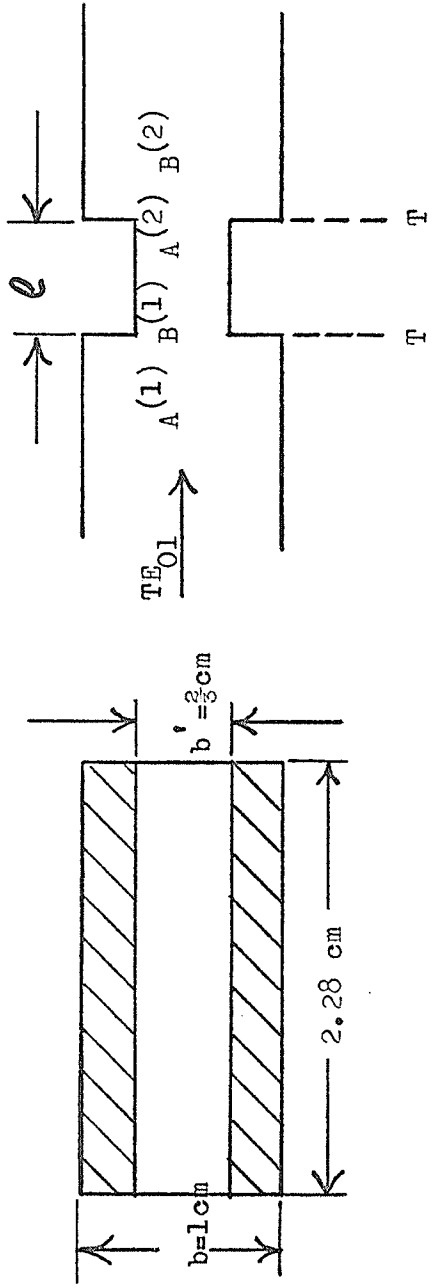


Fig. 4.6 Thick symmetrical iris, end and side view

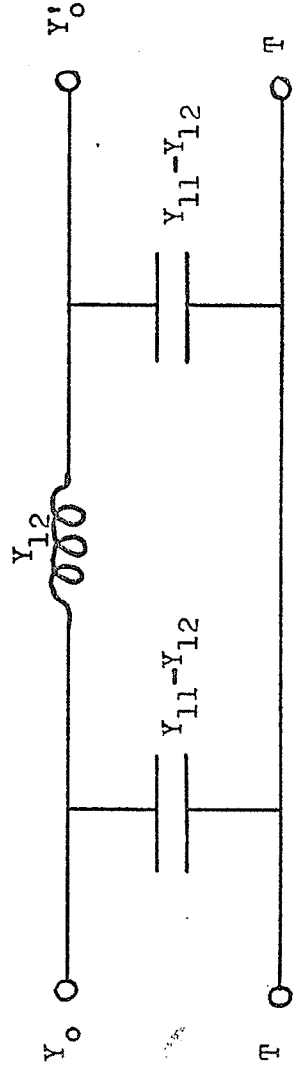


Fig 4.7 Equivalent circuit of thick capacitive iris

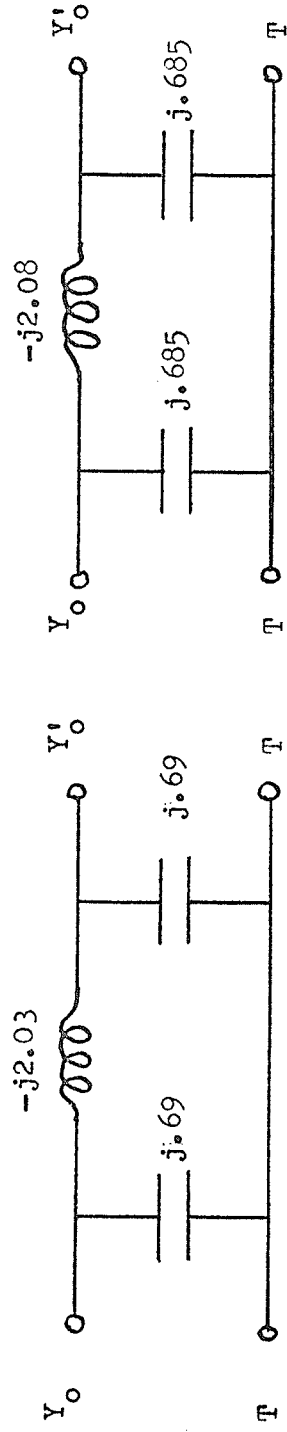


Fig. 4.8 Equivalent circuits from Marcuvitz (17) and modal analysis on right. Thick iris case.

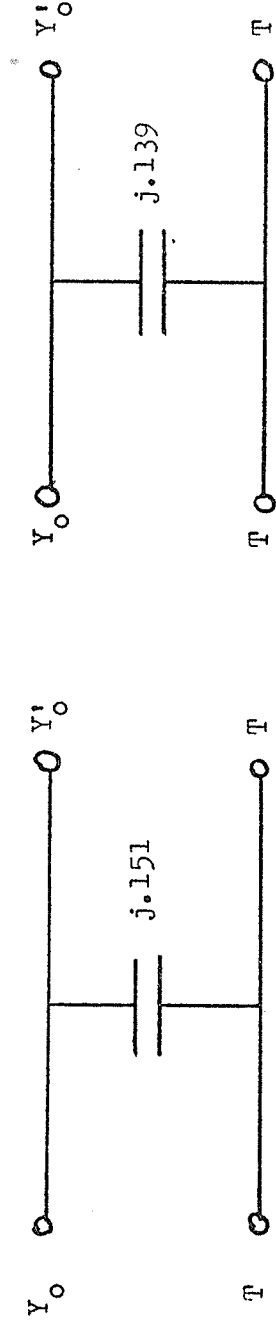


Fig. 4.9 Equivalent circuits from Marcuvitz (17) and modal analysis on right. Thin iris case.

39.

be zero so are not shown. The lower arm member agrees to within

8%.

5 TWO DIMENSIONAL STEP

The combined E and H-plane step is of considerable interest but there are no general analytic techniques available to solve it. The iris composed of two such steps is often used in guides since it can be made to resonate at a particular frequency by a suitable choice of dimensions. Comparison is made with an empirical rule given for the construction of resonant windows. It is shown that it is feasible for the modal analysis method to give the dimensions of a window.

5.1 Mode Types Excited

The two dimensional semi-infinite step is shown in Fig. 5.1. With an incident TE_{01} mode in the z direction, the modes excited on both sides of the junction are TE_{mn} with $m = 0, 1, 2, \dots$ and $n = 1, 2, 3, \dots$ and when $m \neq 0$ TM_{mn} . If there is symmetry about a central axial y-z plane then n is odd. The transverse E and H field patterns for an i-th TE_{mn} and a j-th TM_{mn} mode in guide A(1) are the following:

TE_{mn} modes

$$\bar{e}_{ai} = \frac{j\omega\mu}{k^2_{cmn}} (k_{ym} \cos k_{xm} x \sin k_{yn} y \bar{u}_x - k_{xm} \sin k_{xm} x \cos k_{yn} y \bar{u}_y) \quad (5.1)$$

$$\bar{h}_{ai} = \frac{Y_{mn}}{k^2_{cmn}} (-k_{xm} \sin k_{xm} \cos k_{yn} y \bar{u}_x - k_{yn} \cos k_{xm} x \sin k_{yn} y \bar{u}_y) \quad (5.2)$$

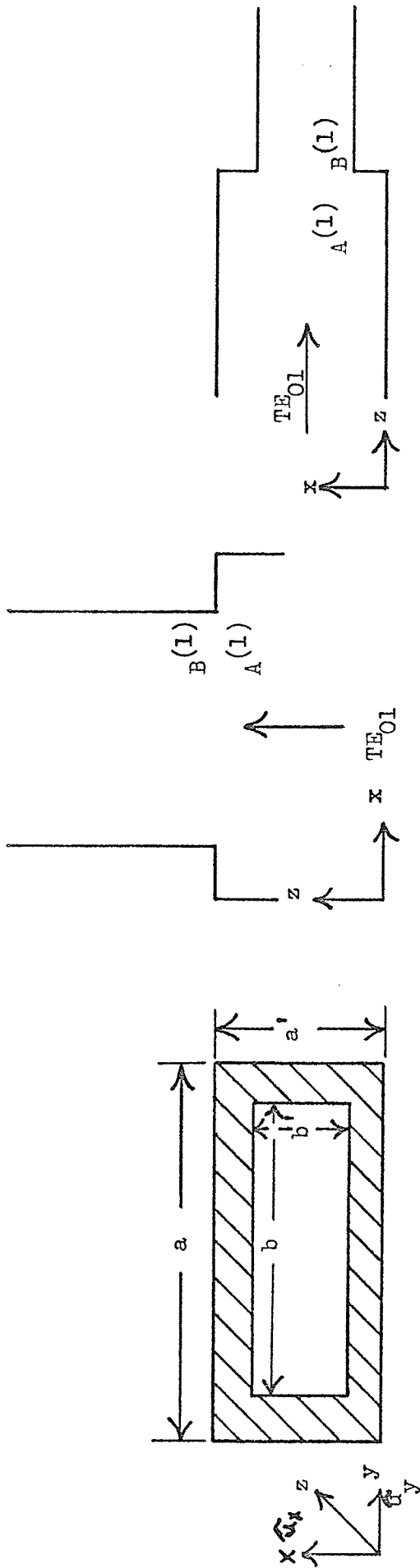


Fig. 5.1 Two dimensional step. End, top and side view

and TM_{mn} modes

$$\bar{e}_{aj} = \frac{\gamma_{mn}}{k_{cmn}^2} (k_{xm} \cos k_{xm} x \sin k_{yn} y \tilde{u}_x + k_{yn} \sin k_{xm} x \cos k_{yn} y \tilde{u}_y) \quad (5.3)$$

$$\bar{h}_{aj} = \frac{j\omega\epsilon}{k_{cmn}^2} (k_{yn} \sin k_{xm} x \cos k_{yn} y \tilde{u}_x - k_{xm} \cos k_{xm} x \sin k_{yn} y \tilde{u}_y) \quad (5.4)$$

where

$$k_{xm} = \frac{m\pi}{a'} \quad k_{yn} = \frac{n\pi}{a}$$

$$\gamma_{mn}^2 = k_{xm}^2 + k_{yn}^2 - \omega^2\mu\epsilon \quad (5.5)$$

$$k_{cmn}^2 = k_{xm}^2 + k_{yn}^2$$

Similar mode field patterns exist in guide B⁽¹⁾ with

$$k_{xm} = \frac{m\pi}{b'} \quad k_{yn} = \frac{n\pi}{b} \quad (5.6)$$

Since each mode has two independent variables describing it, m and n , and for each m and n not zero there are two resulting modes TE_{mn} and TM_{mn} , an ordering system has to be applied. The system used was to call TE_{01} the first mode and increment each m and n to a predetermined m_{max} and n_{max} including the corresponding TM mode if it exists. For example if $m_{max} = 4$ and $n_{max} = 3$ and the junction is completely symmetrical, then m is even and n is odd. The resulting 8 modes are TE_{01} , TE_{03} , TE_{21} , TM_{21} , TE_{41} , TM_{41} , TE_{43} , TM_{43} . By a suitable choice of m_{max} and n_{max} the mode types can be chosen to cater for more or less severe discontinuities in either the E-plane or the H-plane.

5.2 Integral Calculations

The mode types are essentially the same as in Chapter 4, that is, they are two dimensional functions. The double integrations can again be broken into the product of two one dimensional integrals thus saving considerable calculations.

5.3 Semi-infinite Symmetrical Step

The step of Fig. 5.1 is solved for symmetrical cases only with an incident TE_{01} mode. Here the number of modes required to get a good solution is just less than the square of the number of modes needed for a one dimensional step. For this step the number of modes used was 18 with $m_{\max} = 6$ and $n_{\max} = 5$. Since $b = 1.5$ and $b' = 0.8$, the severity of the step was approximately equal in both directions, hence $m_{\max} \approx n_{\max}$. For $f = 13$ GHz. the resulting input admittance is as indicated in Fig. 5.2. This agrees to within 20% of a very approximate method given by Bandler (19) for the same problem. It is interesting to run the same problem with $b = 2.0$, $b' = 0.7$ and $f = 13$ GHz. The resulting equivalent circuit is shown in Fig. 5.3. Because the steps are relatively small, Bandler's (19) approximation method is more accurate and the results agree to within 2%.

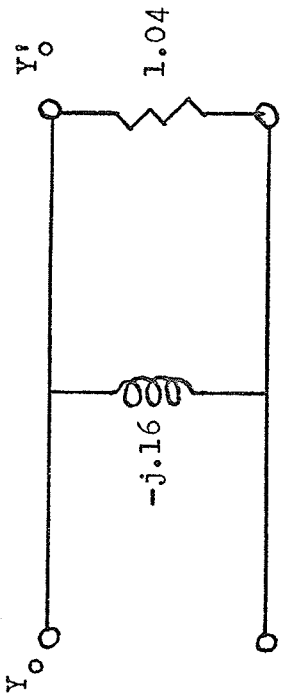


Fig. 5.2 Two dimensional step equivalent circuit with load $b = 1.5$ cm and $b' = .8$ cm.

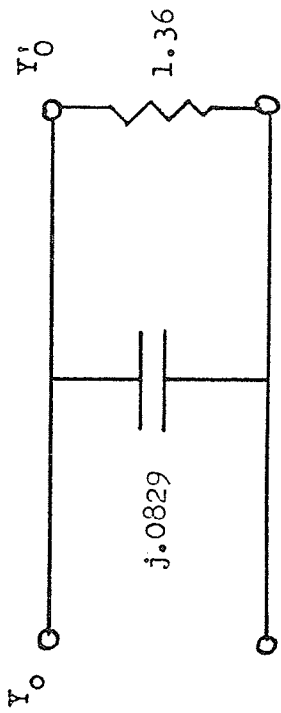


Fig. 5.3 Two dimensional step equivalent circuit with load $b = 2$ cm and $b' = .7$ cm

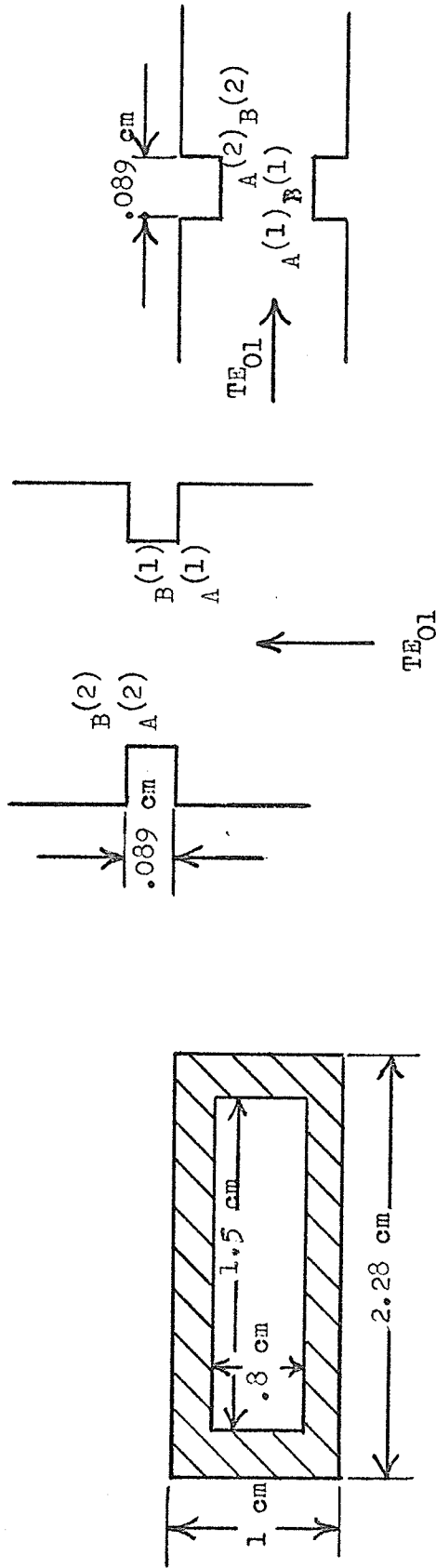


Fig. 5.4 Symmetrical window in waveguide. End, top and side view

These two examples show that this type of step can be either capacitive or inductive depending on the sizes b and b' and also the frequency. The step can be made to resonate at any frequency by the proper choice of parameters. Under this condition the capacitive and inductive components of the step are exactly equal. This leaves no imaginary component.

5.4 Irises

The symmetrical iris or window of Fig. 5.4 is studied by using the single step results of Sec. 5.4. The resonant properties of this particular window are described by Walker (20) and the VSWR is plotted against λ_0 , the free space wavelength, in Fig. 5.5. These are experimental results and are thus for a very slightly lossy system and hence the VSWR does not go to exactly one. For modal analysis results the imaginary parts must exactly cancel and so small errors in determining each part of the impedance, ie. capacitance or inductance, lead to large percentage errors in the resulting resonant frequency.

The resulting input impedance of the window is not constant with the number of modes used but jumps around when the frequency is near resonance. Three VSWR curves corresponding to $M = N = 16, 18,$ and 20 are given in Fig. 5.5. The minima for the curves are centered about the experimental minimum thus indicating that modal analysis can give relatively close answers.

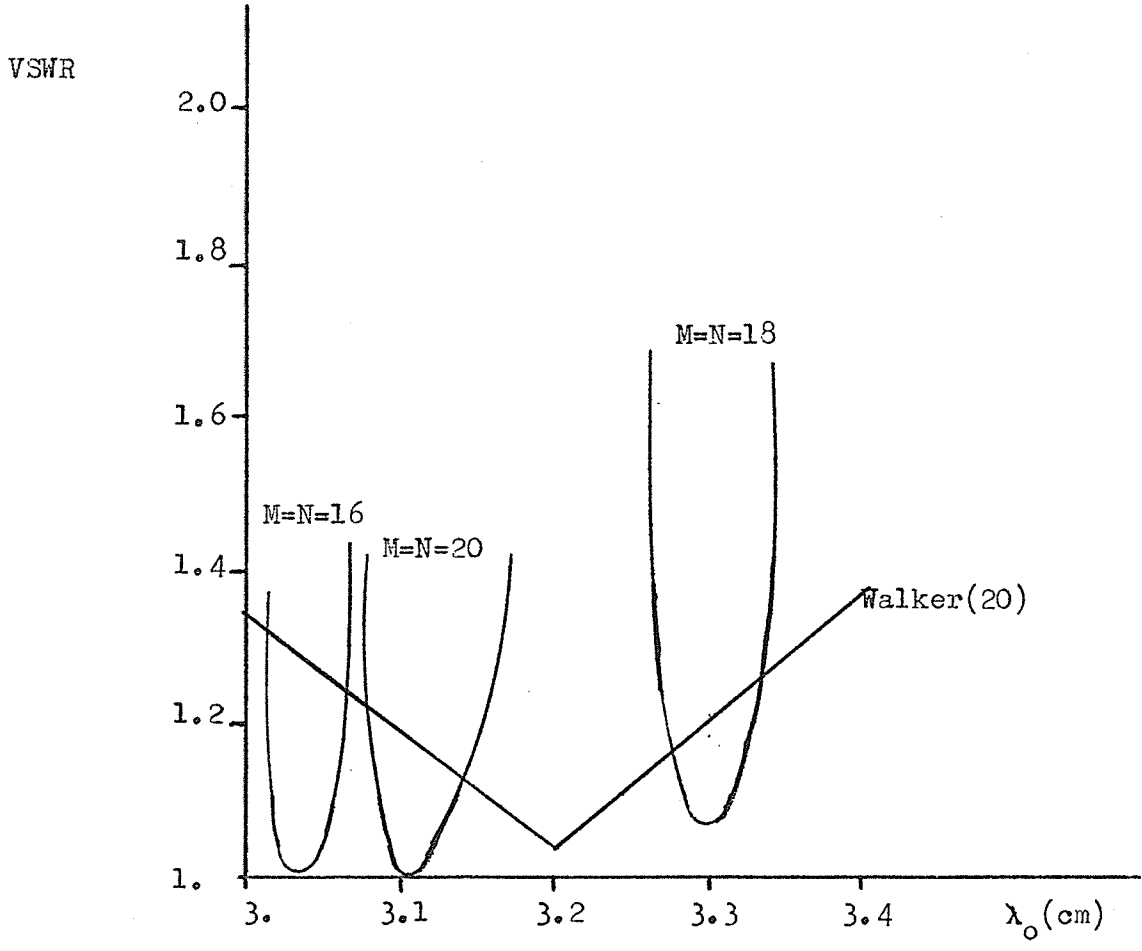


Fig. 5.5 Standing wave ratio of resonant window

6. FIELD SINGULARITIES

The results of the previous chapters have indicated that convergence is rather slow for all configurations when accuracy is desired. The outstanding aspect about the field plots of Chapter 3 is that the H-field goes to infinity near the edge of the discontinuity. A great many modes must be taken into account to accurately reproduce the field. In this chapter a term is introduced to help create the field singularity.

6.1 Numerical Treatment of the Singularity

Fox and Sankar (22) solved a screw propellor problem using finite differences by first ignoring a singularity which was known to occur at a point. The solution showed considerable disturbances at the singularity point and so an alternative method was sought. They composed a special analytic function which was valid only in the neighborhood of the singularity and was completely known in form except for three magnitude coefficients. This function satisfies the differential equation and boundary conditions in the neighborhood of the singularity

point.

The finite difference technique was applied to the problem again; this time leaving out a small region surrounding the singularity. Then the constants of the special expression were solved using three finite difference points. The special function was then used to define the field in the neighborhood of the singularity. This technique provides accurate answers to the problem since they were able to make a comparison with a known analytic solution.

A modification of this technique will be attempted to help the modal analysis method converge to a solution.

6.2 E-Wave on Wedge in Free Space

A wedge in free space is considered next since it will be used in the treatment of waveguide steps. If the right-angled wedge in Fig. 6.1 is in the path of a plane E-wave travelling in the $-y$ direction then the magnetic field near the edge goes to infinity. An E-wave is a polarized plane wave with electric field in the z -direction. There is an edge condition that requires the energy density to be integrable at the edge. While the magnetic field goes to infinity at the edge,

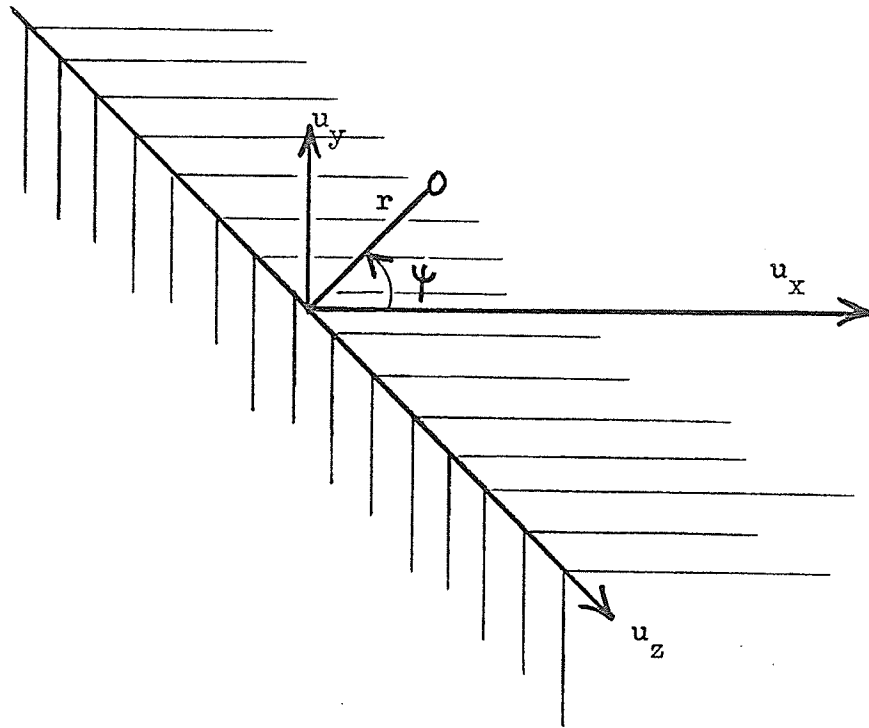


Fig. 6.1 Right angled wedge in free space.

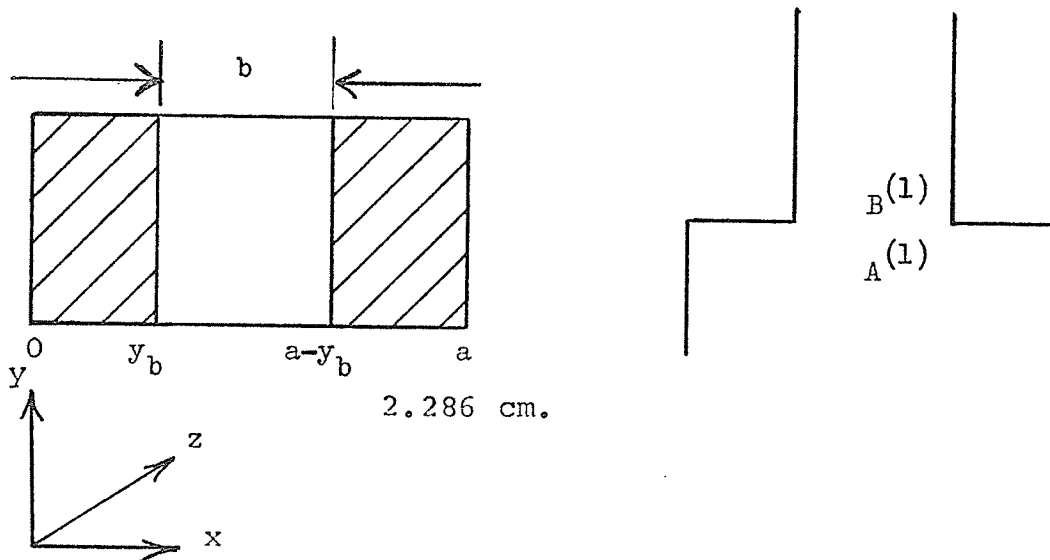


Fig. 6.2 H-plane step end and top view

the electric field remains finite in the vicinity of the edge and vanishes right at the edge. If $r-\psi$ are the polar co-ordinates centered on the wedge edge, the fields in the vicinity of the edge are given by Van Bladel (21) as

$$E_z = A r^{2/3} \sin^{2/3} \psi \quad (6.1)$$

and

$$H_t = -\frac{2}{3} \frac{A}{j\omega\mu} \frac{1}{r^{1/3}} (\tilde{u}_x \cos \psi/3 + \tilde{u}_y \sin \psi/3)$$

These expressions are valid only in free space and are accurate only near the wedge, but they can be used in a stepped waveguide to describe fields very near the edge.

6.3 Special Mode Formulation

The solution of the semi-infinite H-plane step of Ch. 3 is considered again. The step of Fig. 6.2 has two corners in the same orientation as that of Fig. 6.1 with $\psi = 0$ or $\psi = 180^\circ$. By re-writing the electric field part of (6.1) and changing the co-ordinate system to that of the waveguide in Fig (6.2), the E-field near the edge in guide A(1) is represented by a special function E_{Axs}

$$E_{\text{Axs}} = \begin{cases} 3/2 \sqrt{3} j\omega\mu A (y - y_b)^{2/3} & y_b < y < y_b + \delta \\ 3/2 \sqrt{3} j\omega\mu A (a - y_b - y)^{2/3} & a - y_b - \delta < y < a - y_b \\ 0 & \text{Elsewhere} \end{cases} \quad (6.3)$$

The field in this function is defined to be zero if it is not within an arbitrary distance δ of the edge and when it is tangential to the metal. In this study δ was chosen to be 0.1 cm. for the X-band guide of 2.23 cm. The corresponding H-field special function definition is then

$$H_{Ays} = \begin{cases} \frac{A}{(y-y_b)^{\frac{1}{3}}} & y_b \leq y \leq y_b + \delta \\ \frac{A}{(a-y_b-y)^{\frac{1}{3}}} & a - y_b - \delta \leq y \leq a - y_b \\ \frac{2}{\sqrt{3}} \frac{A}{(y-y_b)^{\frac{1}{3}}} & y_b - \delta \leq y < y_b \\ \frac{2}{\sqrt{3}} \frac{A}{(y-a+y_b)^{\frac{1}{3}}} & a - y_b \leq y \leq a - y_b + \delta \end{cases} \quad (6.4)$$

There is a component of the magnetic field tangential to the conductor wall for $\psi = 0^\circ$. These two functions E_{Axs} and H_{Ays} will be treated as one special mode to be used with the other normal waveguide modes.

Any function that is used in the modal analysis technique must be linearly independent of the other functions to be fitted. This is necessary to ensure that the integration of (A.2.1) goes to zero. For this problem the functions E_{sx} and H_{ys} were made orthogonal to the TE_{on} normal waveguide modes by using the Gram-Schmidt procedure to eliminate the mode components in the

special function. This ensures that all functions used are linearly independent since orthogonality guarantees linear independence. If M normal waveguide modes in guide $\Lambda^{(1)}$ are used, then the new orthogonalized special functions are

$$E'_{Axs} = E_{Axs} - \frac{2}{a} \sum_{i=1}^M \sin k_{ai} y \int_a \sin k_{ai} y E_{Axs} dy \quad (6.5)$$

and

$$H'_{Ays} = H_{Ays} - \frac{2}{a} \sum_{i=1}^M \sin k_{ai} y \int_a \sin k_{ai} y H_{Ays} dy \quad (6.6)$$

6.4 Methods of Integrating With Singularities

The integrations in (6.5) and (6.6) are not given in integral tables and thus must be evaluated numerically as described in Sec 3.2. An added complication is that the integrand in (6.6) goes to infinity at two places at the edge along the y -axis while the integration along the axis is finite. A direct numerical technique fails since the derivative also goes to infinity at these two places and a finite number of evaluations of the integrand near the edge do not give the resulting integral. The contribution to the integral very near the singularity goes to zero and thus this point may be omitted. The region omitted was arbitrarily chosen as the smallest distance that the word length

of the computer used would allow. The region omitted was 10^{-5} cm. wide and using the Simpson's rule integration technique, results were obtained.

There are however other numerical methods which remove the singularities from the domain of the integrand. Of the four methods suggested by Froberg (23), the substitution method is applicable here. The integrations are carried out only in the vicinity of the edge and so part of the integral of (6.6) becomes

$$\frac{2}{\sqrt{3}} \int_{y_b-\delta}^{y_b} \frac{\sin k_{ai} y}{(y-y_b)^{1/3}} dy = \frac{-2}{\sqrt{3}} \int_{.1}^0 \frac{\sin k_{ai} (y_b-y)}{y^{1/3}} dy \quad (6.7)$$

Let $y=t^3$ in (6.7) and we have

$$\frac{-2}{\sqrt{3}} \int_{\sqrt[3]{.1}}^0 \sin[k_{ai} (y_b-t^3)] t dt \quad (6.8)$$

The integrand of (6.7) has a singularity while (6.8) has none and the derivatives are regular also. The numerical integration technique was then applied to (6.8) to arrive at the results of Table 6.1.

Special functions are defined for the junction in guide B(1), but here both the electric and magnetic field exist only for $\psi = 180^\circ$ in the plane of the junction. The special fields are given as

$$E_{Bxs} = \begin{cases} \frac{3}{2} \sqrt{3} j \omega \mu A y^{2/3} & y \leq \delta \\ \frac{3}{2} \sqrt{3} j \omega \mu A (b-y)^{2/3} & y \geq b - \delta \\ 0 & \text{Elsewhere} \end{cases} \quad (6.10)$$

and

$$H_{Bys} = \begin{cases} \frac{A}{y^{\frac{1}{3}}} & y \leq \delta \\ \frac{A}{(b-y)^{\frac{1}{3}}} & y \geq b - \delta \end{cases} \quad (6.11)$$

As with the functions in the $A^{(1)}$ guide, these special functions have to be made orthogonal to the $B^{(1)}$ guide normal waveguide modes. This is done by

$$E'_{Bxs} = E_{Bxs} - \frac{2}{b} \sum_{i=1}^N \sin k_{bi} y \int_b \sin k_{bi} y E_{bxs} dy \quad (6.12)$$

$$H'_{Bys} = H_{Bys} - \frac{2}{b} \sum_{i=1}^N \sin k_{bi} y \int_b \sin k_{bi} y H_{bys} dy \quad (6.13)$$

where N is the number of normal modes used in waveguide $B^{(1)}$.

If the number of normal modes is nine, and one special mode is used, then the nine coefficients of the $\sin(k_{ai}y)$ and $\sin(k_{bi}y)$ terms are given in Table 6.1 for the special functions in the form

$$E'_{Axs} = E_{Axs} - \sum_{i=1}^M E_{Ai} \sin k_{ai} y \quad (6.14)$$

$$H'_{Ays} = H_{Ays} - \sum_{i=1}^M H_{Ai} \sin k_{ai} y \quad (6.15)$$

$$E'_{Bxs} = E_{Bxs} - \sum_{i=1}^N E_{Bi} \sin k_{ai} y \quad (6.16)$$

$$H'_{Bys} = H_{Bys} - \sum_{i=1}^N H_{Bi} \sin k_{ai} y \quad (6.17)$$

These functions can be used in the modal analysis method since

i	E_{Ai}	H_{Ai}	E_{Bi}	H_{Bi}
1	.01729	.8651	.07715	.12373
2	.01132	.8525	.02184	.35454
3	-.02088	-.7944	.03231	.53853
4	-.00399	-.7874	.03754	.65443
5	.02152	.6802	.03699	.69359
6	-.00343	.6714	.03127	.66103
7	-.01923	-.5308	.02192	.57363
8	.00968	-.5237	.01109	.45599
9	.01457	.3697	.00099	.33487

Table 6.1 Coefficients to orthogonalize special functions from (6.14) to (6.17). For wedge.

they are now linearly independent of the normal waveguide modes.

6.5 Modified Solution of H-Plane Step

The H-plane step is solved using nine regular waveguide modes and the functions (6.14)-(6.15) and (6.16)-(6.17) as one mode each. The first step is to calculate the integrals of (1.7) to (1.9) which involve these special functions. The method of calculation was essentially the same as described in Sec. 6.4. Using these values plus the regular integrals, a solution to the step is obtained by the modal analysis method. The results are compared with the results for $M = N = 10$ and 15 for $f = 10$ GHz. using normal waveguide modes. Two results from Table 3.1 are summarized here along with the special function solution.

$$Y = -j2.323 \quad M = N = 10$$

$$Y = -j2.330 \quad M = N = 15$$

$$Y = -j2.328 \quad \text{special } M = N = 9$$

The magnitudes of the H-field at the junction are plotted for this solution in Fig. 6.3. For comparison purposes the corresponding plot of the magnetic field match from Fig. 3.4 for $M = N = 15$ is shown above it. As can be seen the field match near the metal edge is very close as compared to the normal mode method. There is however a mismatch in field values where the special function starts on each side of the metal edge. The effect of the special function on the electric field is small and

there is no difference in the already near perfect electric field match and for this reason it is not plotted.

Assuming that the normal solution for $M = N = 15$ is more accurate than the normal solution for $M = N = 10$, one can see a slight improvement using the special mode formulation. The result does not, however, appear as accurate as the $M = N = 15$ case. To clarify the potential of the special mode method to give improved results, tests were run on the semi-infinite symmetrical bifurcation for which an exact solution is known.

6.6 Modified Solution of the H-Plane Bifurcation

The semi-infinite H-Plane bifurcation shown in Fig. 6.4 was solved by Wexler(24), using modal analysis. The solution for a large number of modes compared favorably with the exact solution given by Marcuvitz(25).

To derive a special function needed for this solution, consider an incident E-wave on the thin edge with electric field parallel to the edge in Fig. 6.5. The solutions for the fields near the edge are again given by Van Bladel(26) as

$$E_z = A r^{1/2} \sin \psi / 2$$

(6.18)

$$H_t = - \frac{A}{2j\omega\mu r^{1/2}} (u_x \cos \psi / 2 + u_y \sin \psi / 2)$$

These equations are quite similar to (6.1), since here also the

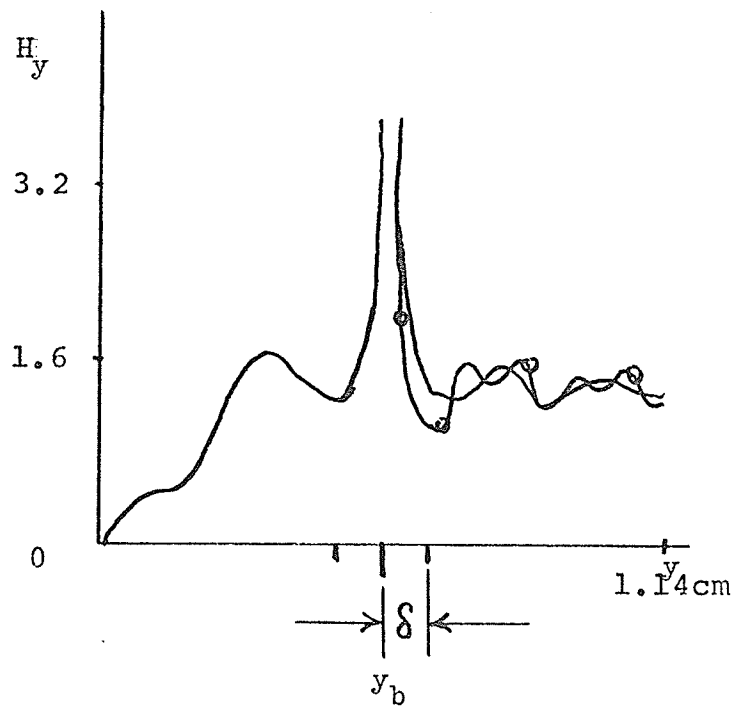
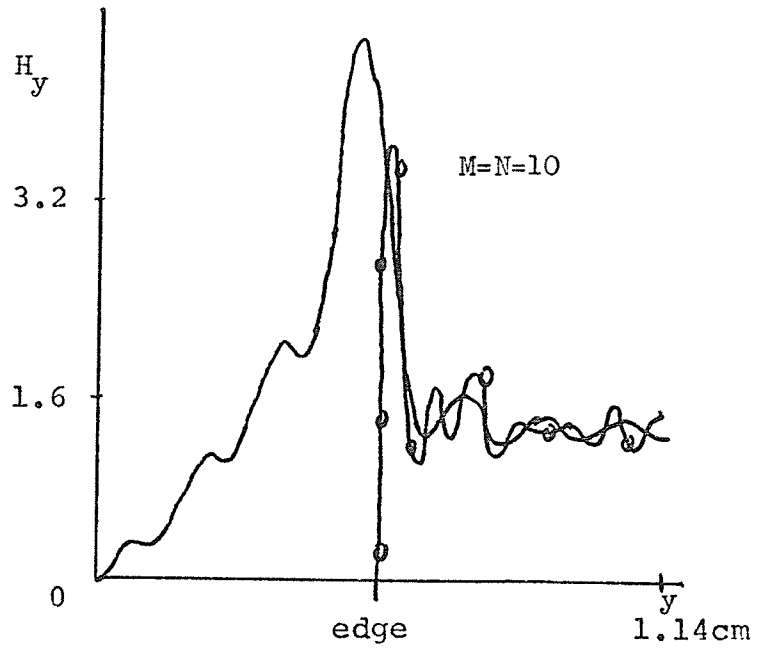


Fig. 6.3 Magnitude of magnetic field showing match with modal method above and special function method below

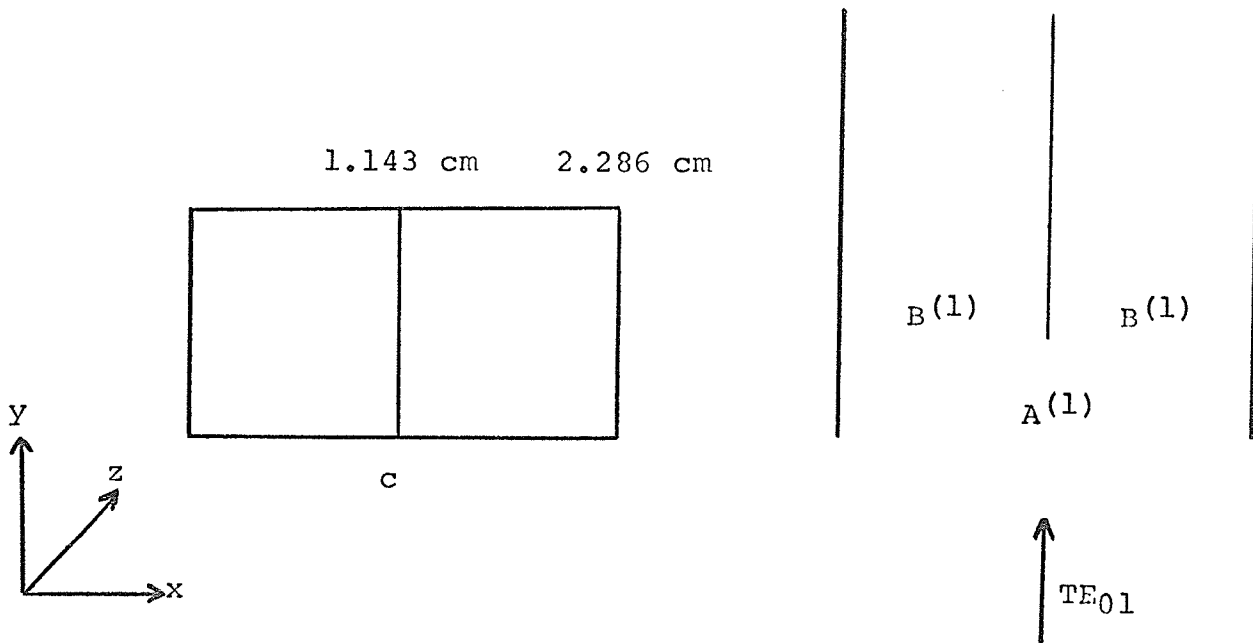


Fig. 6.4 H-Plane bifurcation, end and top view.
Guide B is in cutoff.

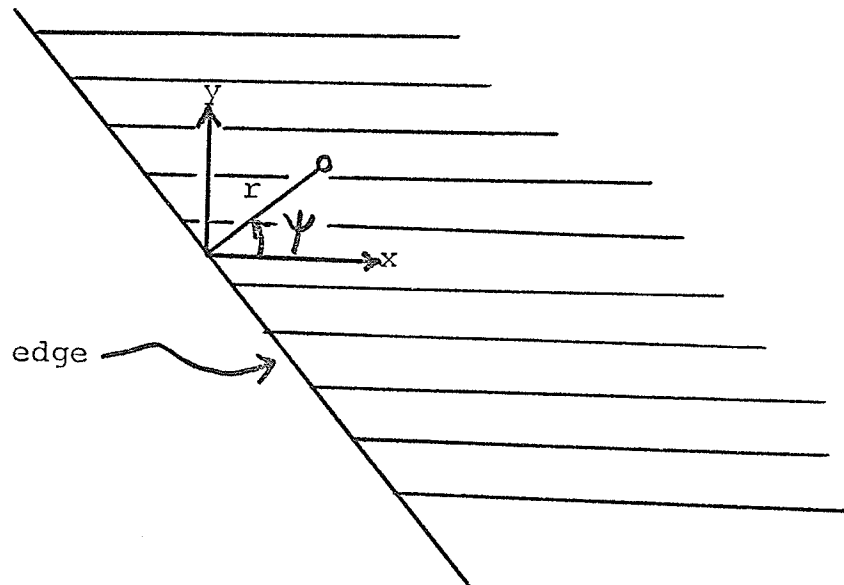


Fig. 6.5 Thin edge with coordinate system.

H-field must go to infinity at the edge and the E-field goes to zero at the edge.

By re-arranging (6.18) and changing the co-ordinate system to that of Fig. 6.4, the functions used in the waveguide become

$$\begin{array}{ll} 2j\omega\mu A(c-y)^{\frac{1}{2}} & c-\delta \leq y \leq c \\ 0 & \text{Elsewhere} \end{array} \quad (6.19)$$

and

$$\begin{array}{ll} \frac{A}{(c-y)^{\frac{1}{2}}} & c-\delta \leq y \leq c \\ 0 & \text{elsewhere} \end{array} \quad (6.20)$$

These correspond to the special functions for the wedge which were given in (6.3) and (6.4). The angle ψ was taken as -90° and since the guide is completely symmetrical about the center c , the function is shown only for the left half of the guide. Similar expressions exist for the right hand side but are not used since all calculations are done on the left side only and then multiplied by two.

The corresponding functions used in guide B⁽¹⁾ are exactly the same as (6.19) and (6.20) since the bifurcation has zero width.

The functions in (6.19) and (6.20) are orthogonalized to the normal waveguide modes in exactly the same way as (6.3) and (6.4) were done by using (6.5) and (6.6). The procedure for $B^{(1)}$ guide is done by using (6.12) and (6.13), but substitute E_{Axs} for E_{Bxs} , and H_{Ays} for H_{Bys} as defined in (6.19) and (6.20).

Table 6.2 gives the resulting coefficients as defined in (6.14) to (6.17). It was pointed out by Wexler(27), that for TE_{01} excitation, the normal modes in guide $A^{(1)}$ are odd while the modes in $B^{(1)}$ are both odd and even with the same mode form defined over both $B^{(1)}$ sections.

The functions (6.14) to (6.17) are used as one mode in each guide with the summation taken over the number of normal modes used in each guide. Results were obtained for four and nine normal waveguide modes, to give a total of five and ten terms respectively.

The exact solution for the distance d of the shift of a short circuit equivalent circuit, from the plane of the discontinuity, is given by Marcuvitz(25) and is computed by

$$\frac{2\pi d}{\lambda_g} = \frac{2a}{\lambda_g} (1 + \ln \frac{1}{2}) - S_2 \left(\frac{2a}{\lambda_g}; 1, 0 \right) + 2S_1 \left(\frac{a}{\lambda_g}; \frac{1}{2}, 0 \right) \quad (6.21)$$

where

$$S_N(x; \alpha, 0) = \sum_{n=N}^{\infty} \sin^{-1} \frac{x}{\sqrt{n^2 - \alpha^2}} - \frac{x}{n} \quad (6.22)$$

i	E_{Ai}	H_{Ai}	E_{Bi}	H_{Bi}
1	.03674	1.1046	.01208	.20170
2	-.03556	-1.0880	-.02366	-.39691
3	.03325	1.0555	.03426	.57945
4	-.02992	-1.0085	-.04344	-.74376
5	.02574	.94892	.05087	.88511
6	-.02089	-.87912	-.05627	-.99992
7	.01561	.80192	.05948	1.08568
8	-.01012	-.72030	-.06044	-1.14133
9	.00468	.63736	.05923	1.16718

Table 6.2 Coefficients to orthogonalize special function using (6.14) to (6.17) for thin edge.

and

$$y_{\lambda} = \frac{\lambda}{\sqrt{1 - \left(\frac{\lambda}{2a}\right)^2}}$$

where λ is the free space wavelength.

For a frequency corresponding to $\frac{a}{\lambda} = .7$ the normalized input admittance at the junction was calculated from (6.21) to be $y = 2.4175$. This value differs by 0.002 from the value given by Wexler(28). The infinite summation in (6.22) was terminated when the terms made no difference to the answer.

The solutions using the modal analysis method with the special function are summarized in Table 6.3 along with the solution using modal analysis with normal modes only.

The improvement using the special function for five terms is substantial but the improvement using ten terms is only a little better than using ten normal modes.

One would expect nearly perfect results by using the special function along with normal modes, since the function space spanned by the set used should be nearly complete as far as representing the fields. One improvement may be realized by using a function that represents the singularity across the whole guide width, rather than in the neighborhood of the singularity only. This would require using a power series rather than the first term which dominates near the discontinuity.

no. of terms	normal modes only	with special function
5	-j2.363	-j2.389
10	-j2.396	-j2.401
20	-j2.410	
40	-j2.415	
Exact		-j2.4175

Table 6.3 Normalized admittance at the bifurcation.
 Frequency corresponds to $\frac{a}{\lambda} = .7$ and guide
 width $a = 2.286$ cm.

This would however bring up the complication that the electric field at the guide wall would not be zero as is required by the boundary conditions. However the normal modes may combine to approximate a zero field. This would add computations but in fact may save time in the end since it may permit fewer modes.

These examples demonstrate that using non-orthogonal functions is possible and can give improved results. Perhaps some other functions could be used to give better results.

7. DISCUSSION AND CONCLUSIONS

The modal analysis formulation presented by Wexler apparently converges for any reasonable M/N ratio. The method converged for all step sizes attempted as opposed to the other modal formulation of Clarricoates and Slinn (2), which converge for only one ratio for a given geometry.

The use of a scattering matrix here allows for the solution of multi-junction problems while other formulations given do not allow complicated back scattering from discontinuities on the load side of the junction being solved.

The more accurate Simpson's $1/3$ rule (23) could be used for all the integrations if the number of strips required for the desired accuracy were known beforehand. This is not usually the case but when a configuration is used over again many times with only minor changes in parameters, the $1/3$ rule would give slightly faster integral calculations.

Transverse field plots generally show how a solution has converged but it is not possible to assess how accurate the resulting reflection coefficient is. Usually a good indication can be obtained by running tests on a junction, varying the number of modes used and noting the change in the reflection coefficient ρ . The error is likely to be less than the difference

of the two cases with the highest modes.

The same applies to irises providing they are not too thin. To determine the number of modes required for a relatively thin iris is much harder, since the sequence formed by increasing the number of modes used converges very slowly. There seems to be no way to determine the accuracy of the results obtained without comparison to a known solution.

For configurations which have excited modes that are two dimensional functions, the test for convergence must include jumps in modes used that include modes from the next group along an axis. For example if TE_{87} was the highest mode for a trial run then the next highest mode number to use must include the TE_{98} mode.

The formulation given for the field singularity appears to give improved results for the same number of modes. The method used was quite cumbersome and it was not easy to run test cases varying the number of modes used. A real test of its worth would be in the two dimensional step where convergence was a real problem. This would necessitate the inclusion of a term for the electric field since for the E-plane step the electric field has a singularity at the edge.

APPENDIXA.1 Program Description

The program consists of a main calling program which calls nine subroutines which in turn use eleven function subprograms. The calling sequence is given in Fig A.1 and a description of each subprogram follows.

The main program declares many of the variables used throughout the program and are thus stored in common. The parameters of the first junction to be solved are read in. Waveguide parameters are calculated which are necessary for the placement of short and open circuit terminations, and then the scattering matrix for the first junction to be solved is assembled. Subroutine CNTRL is then called and data for the next junction is read. Then the reflection coefficient is printed for the previous junction and these last three steps are repeated until all junctions are solved.

Subroutine CNTRL is simply a sequence of calling statements which call MATS, SIMCOM, SLVEQ, and BASC in that order.

Subroutine MATS is a routine which computes all the integrals and scattering matrices required by the program. It also calls GAM to get mode types and characteristics. MATS also

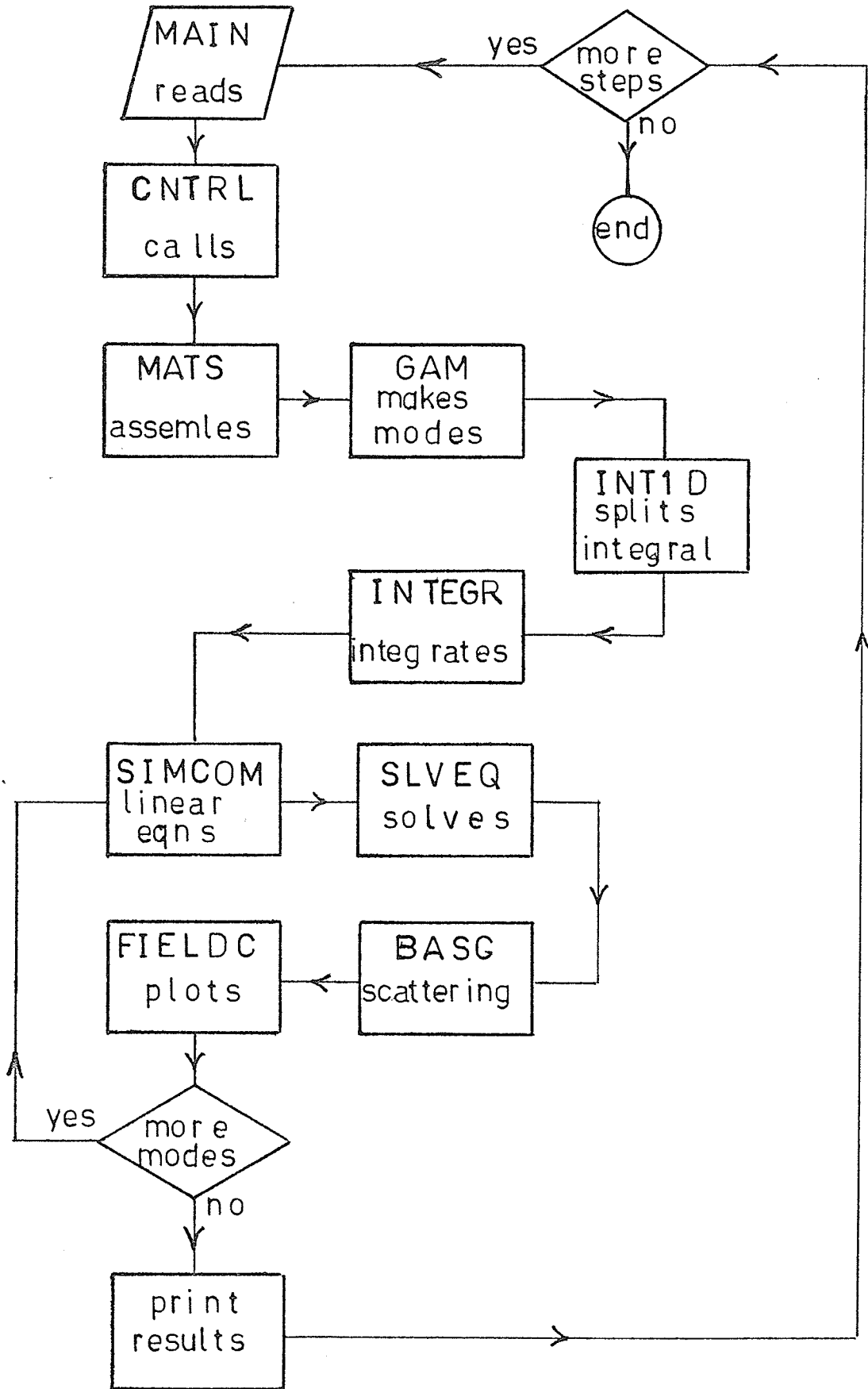


Fig. A1 Flow chart of modal analysis program

calls routines TF for field plots, and INT1D to carry out the integrations.

Subroutine GAM generates the necessary modes and their propagation constants for particular junction geometrys.

TF is used, when desired, to produce a map of the field value contributions of each mode used. It is used in conjunction with subroutine FIELDDC to sum up the actual fields after the coefficients are known. Both these subroutines are used only for plotting purposes and are not necessary for the junction solution.

Subroutine INT1D is a routine which breaks two dimensional integrations into one dimensional integrations. It calls the routine INTEGR to perform the actual integrations of the functions F1, F2, F3, ..., F8.

SIMCOM takes the results of the integrations from MATS and produces a set of complex linear equations according to (1.5 - 1.12). These equations are solved by subroutine SOLVEQ which uses complex elimination with partial pivoting. The solution vector is printed out and next subroutine BASC is called. This routine calculates the back scatterings coefficients according to (1.13). If field plots are desired then FIELDDC is called next.

```

0001 REAL LAMBDA,LENGTH,KXA(30),KYA(30),KCASC(30),KSC,MU/12.56637E - 9/      'CC1C
0002 INTEGER R,RMIN,RMAX,FJCN,XXSYM,YSYM                                     0020
0003 DATA C/29.97925/,TWCPI/6.283185/,EPSLNC/8.8542E - 14/              CC3C
0004 INTEGER SHORT/'SC'/,CPEN/'CC'/,MATCH/'ML'/                            C04C
0005 COMPLEX A(30),AVEC(30,30),B(30),CD(30,30),COEF(31,31),RHC,S(30,30)   CC50
&,VEC(31),Y,GAMA(30)                                                    CC60
0006 EQUIVALENCE (RHO,AVEC(1,1))                                           C070
0007 INTEGER*2 MCEA(3,30)                                                  C080
0008 COMMON A,B,CC,S,CCEF,VEC,AVEC,M,N,NP1,R,RMIN,RMAX,CLASS,FJCN,JCN     CC9C
0009 COMMON /MATCOM/GAMA,MODEA,KXA,KYA,KCASC,CMEGA,KSC,XA,YA,XB,YB,APRM    0100
&,ADPRM,BPRM,BCPRM,SML,XXSYM,YSYM,MPM,MDPM                               C11C
0010 COMMON /FACTN/I,J,YYB,YBCPRM                                         C120
0011 10 READ (5,20) XA,YA,APRM,ADPRM,XB,YB,BPRM,BCPRM,LENGTH,CLASS,LOAD,  0130
&NJCN,S,F,M,N,MPM,MDPM,XXSYM,YSYM,FJCN                                  C14C
0012 IFL=F                                                                    C15C
C-----SET UP INTEGER FREQUENCY IN GHZ.                                  0160
0013 DO 120 IF=IFL,IFL                                                       C17C
C F=IF                                                                        C18C
0014 REWIND 4                                                                  0190
C-----R IS THE INCIDENT MODE NUMBER                                       C200
0015 RMIN=1                                                                    0210
0016 RMAX=1                                                                    0220
CC17 IF (NJCN .GT. 1) RMAX=R                                                  0230
0018 20 FORMAT (4F10.1/4F10.1/2F10.1,3X,A2,I5,F10.1/7I5)                 C240
0019 LAMECA=C/F                                                                C250
0020 WRITE (6,30) XA,YA,APRM,ADPRM,XB,YB,BPRM,BCPRM,LENGTH,CLASS,LOAD,   C26C
&NJCN,S,F,M,N,MPM,MDPM,XXSYM,YSYM,FJCN                                  0270
0021 30 FORMAT ('OXA='F8.4,4X,'YA='F8.4,4X,4HA'='F8.4,4X,4HA'='F8.4,4X,'  C280
&XB='F8.4,4X,'YB='F8.4,4X,4HB'='F8.4,4X,'B'='F8.4/' LEN='F7.3,      C290
&SX,'CLASS='F4.1,5X,'LOAD='A2,I8,' JUNCTICNS'5X,'F='F6.2,5X,5X,'M =   0300
&'I3,5X,'N='I3,5X,'M'='I2/' M'='I2,5X,'XXSYM='I1,5X,'YSYM='I1,5X     C310
&'FJCN='I1)                                                                C320
C-----SET ANGULAR FREQUENCY                                               0330
CC22 CMEGA=TWCPI*F*1.E9                                                       C340
C-----CALCULATE GUIDE WAVELENGTHS                                         0350
0023 SUA=1. - (LAMBDA/2./ADPRM)**2                                           C360
0024 SUB=1. - (LAMECA/2./BDPRM)**2                                           C370
0025 GLAMA=LAMBDA/SIGN(SQRT(ABS(SUA))),SUA)                                    C380
0026 GLAMB=LAMECA/SIGN(SQRT(ABS(SUB))),SUB)                                    C390
0027 WRITE (6,40) GLAMA,GLAMB,LAMECA                                         C400
0028 40 FORMAT (' LAMBDA G A='G12.5,' LAMBDA G B='G12.5,' LAMECA='G12.5   0410
&)                                                                            C420
0029 KSC=CMEGA*CMEGA*ML*EPSLNC                                               C430
0030 NP1=N + 1                                                                  C440
0031 SML=LENGTH                                                                C450
C-----DETERMINE LOAD TYPE FOR FIRST JUNCTION SOLVED                       C460
C-----AND WHERE TO PLACE SHORT                                             C470
0032 IF (LCAC .EQ. CPEN) SML=GLAMB/4.                                         C48C
0033 IF (LOAD .EQ. SHORT) SML=GLAMB/2.                                        C49C
0034 IF (LCAC .NE. MATCH) PRINT 5C,SML                                        050C
0035 5C FORMAT (' SHORT AT'G15.5,'CM.')                                       C51C
C-----SET SCATTERING MATRIX TO C FOR MATCHED LOAD AND -1 ON DIAGONAL    0520
C-----FOR SHORT                                                            0530
CC36 DO 7C I=1,N                                                              C54C
0037 DO 6C J=1,N                                                                C550
0038 AVEC(I,J)=(0.,0.)                                                         0560
CC39 IF (LOAD .NE. MATCH) AVEC(I,I)=(- 1.,0.)                               C57C
0040 70 CONTINUE                                                                0580
0041 CC 11C JCN=1,NJCN                                                         C590
C-----SOLVE EACH JUNCTION IN LCCP                                          0600

```

0042	CALL CNTRL	C610
0043	Y=(1. - RFO)/(1. + RHO)	0620
C044	WRITE (6,80) RHC,Y	C630
0045	80 FORMAT ('CRHC = '2G16.8,5X,'Y = '2G16.8)	0640
0046	IF (NJCNS .EQ. 1) GO TO 110	0650
	C-----SET PARAMETERS IN FIRST JUNCTION	C660
0047	RMAX=1	C670
C048	XB=XA	C680
CC49	YB=YA	C690
C050	BPRM=APRM	0700
0051	BCPRM=ACPRM	0710
	C-----READ PARAMETERS FOR NEXT JUNCTION	C720
0052	READ (5,100,END=120) XA,YA,APRM,ACPRM,SML,CLASS	C730
C053	PRINT 90,XA,YA,APRM,ADPRM,SML,CLASS	0740
C054	90 FORMAT ('CXA',T16,'YA',T32,'APRM',T48,'ADPRM',T64,'LENGTH',T80,'CL CLASS',/6G16.6)	C750
0055	100 FORMAT (4F10.1/2F10.1)	0760
C056	110 CONTINUE	0770
CC57	120 CONTINUE	C780
0058	130 CALL EXIT	C790
CC59	END	0800
		C810

0001		SUBROUTINE CNTRL	CC10
	C-----	CALLS SUBROUTINES FOR EACH INCIDENT MODE	CC20
0002		REAL LAMBDA	CC30
0003		INTEGER R,RMIN,RMAX,FJCN	0040
0004		COMPLEX A(30),AVEC(30,30),B(30),CD(30,30),COEF(31,31),PRHO,S(30,30	CC50
		E),VEC(31),Y,D	CC60
0005		COMMON A,B,CC,S,CCEF,VEC,AVEC,M,N,NP1,R,RMIN,RMAX,CLASS,FJCN,JCN	0070
0006		CALL MATS	CC80
0007		DO 10 R=RMIN,RMAX	CC90
0008		CALL SIMCOM	0100
0009		CALL SLVEC(CCEF,VEC,NP1,31,D,6)	C110
0010	10	CALL BASC	C120
0011		PRINT 20,(VEC(I),I=2;NP1)	0130
0012	20	FORMAT (//(' BJ'2G16.8))	C140
0013		PRINT 30,(AVEC(I,1),I=1,M)	0150
0014	30	FORMAT (//(' AI'2G16.8))	C160
0015		BJ=CABS(VEC(2))	C170
0016		AI=CABS(AVEC(1,1))	C180
0017		PRINT 40,BJ,AI	0190
0018	40	FORMAT (//(' B1 = 'G15.7,' R+C = 'G15.7)	C200
0019		IF (FJCN .NE. C) CALL FIELDG(VEC,AVEC,M-1,N)	0210
	C-----	M-1 FOR SPECIAL MODE ONLY	0220
0020		RETURN	0230
0021		END	0240

```

0001      SUBROUTINE MATS
0002      COMPLEX A(30),AVEC(30,30),B(30),CD(30,30),COEF(31,31),S(30,30),VEC
&(31),GAMA(30),GAMB(30),CLMNY,GA,GL
0003      INTEGER*2 MODEA(3,30),MCDEB(3,30),TE/'TE'/,TM/'TM'/
0004      EXTERNAL F1,F2,F3,F4,F5,F6,F7,F8
0005      EXTERNAL FSE,FSH,FD
0006      REAL KSC,KXA(30),KXB(30),KYA(30),KYB(30),KCASC(30),KCBSQ(30),INTID
&,MU/12.56637E-9/,INT
0007      DATA PI/3.141593/,EFSLCN/8.8542E-14/
0008      INTEGER HM,HMP1,HN,HNP1,XYM,YSYM,SPACE(4)
0009      COMMON A,B,CD,S,CCEF,VEC,AVEC,M,N,SPACE,CLASS,FJCN
0010      COMMON /MATCCM/GAMA,MODEA,KXA,KYA,KCASC,CMEGA,KSC,XA,YA,XB,YB,APRM
&,ADPRM,EPRM,BDPRM,SML,XYM,YSYM,MPMAX,MDPMAX
0011      COMMON /FACTN/I,J
0012      COMMON /GB/KXB,KYB,KCBSQ
0013      COMMON CEXP
0014      C....PRECEDING CARD FOR WATFIV ONLY
      READ IC,NM
0015      C-----SET NM=M FOR SPECIAL MCDE FORMULATION ONLY
      10  FORMAT (I2)
0016      C-----SET UP MCDE TYPES FOR THE TWO GUIDES AT THE JUNCTION
      CALL GAM(MPMAX,MDPMAX,XYM,YSYM,KSQ,APRM,ADPRM,GAMA,MODEA,NN)
0017      CALL GAM(MPMAX,MDPMAX,XYM,YSYM,KSQ,BPRM,BDPRM,GAMB,MODEB,NN)
0018      C-----CHECK TO SEE HOW MANY MODES GENERATED
      IF (M.NE.NN) PRINT 20,NN
0019      20  FORMAT (' # MODES='I2)
0020      DO 50 J=1,M
0021      I=J
0022      C-----CALCULATE MODE PATTERNS FOR BOTH GUIDES
      KXA(J)=PCCEA(1,J)/APRM*PI
0023      KYA(J)=PCDEA(2,J)/ADPRM*PI
0024      KCASC(J)=KXA(J)*KXA(J) + KYA(J)*KYA(J)
0025      KXB(J)=PCCEB(1,J)/BPRM*PI
0026      KYB(J)=PCDEB(2,J)/BDPRM*PI
0027      KCBSQ(J)=KXB(J)*KXB(J) + KYB(J)*KYB(J)
0028      IF (MCDEB(3,J).EQ.TM) GC TC 40
0029      C-----CALCULATE INTEGRATIONS
      AP=KXA(J)*INTID(F1,F1,F2,F2,XA,XA + APRM,YA,YA + ADPRM)*KXA(J)
0030      ADP=KYA(J)*INTID(F3,F3,F4,F4,XA,XA + APRM,YA,YA + ADPRM)*KYA(J)
0031      A(J)=(C.,1.)*OMEGA/KCASC(J)*MU/KCASC(J)*GAMA(J)*(AP + ADP)
0032      BP=KXB(J)*INTID(F5,F5,F6,F6,XB,XB + BPRM,YB,YB + BDPRM)*KXB(J)
0033      BDP=KYB(J)*INTID(F7,F7,F8,F8,XB,XB + BPRM,YB,YE + BDPRM)*KYB(J)
0034      B(J)=(C.,1.)*OMEGA/KCBSQ(J)*MU/KCBSQ(J)*GAMB(J)*(BP + BDP)
0035      C-----SET UP FIELD PATTERN IN A GUIDE
      C-----E FIELD IN A
      IF (FJCN.NE.0.AND.J.LT.NM) CALL TF((C.,1.)*OMEGA*MU*KYA(J)/
&KCASC(J),XA,YA,F3,F4)
0036      C-----H FIELD IN A
      IF (FJCN.NE.0.AND.J.LT.NM) CALL TF((1.,0.)*GAMA(J)/KCASC(J)*
&KYA(J),XA,YA,F3,F4)
0037      GO TO 3C
0038      IF (FJCN.NE.0.AND.J.EQ.NM) CALL TF((C.,1.)*OMEGA*MU*1.5*SQRT
&(3.),XA,YA,FC,FSE)
0039      IF (FJCN.NE.C.AND.J.EQ.NM) CALL TF((1.,0.),XA,XA,FC,FSH)
0040      C-----E FIELD IN B
      30  IF (FJCN.NE.0.AND.J.LT.NM) CALL TF((0.,1.)*OMEGA*MU*KYB(J)/
&KCBSQ(J),XB,YB,F7,F8)
0041      C-----H FIELD IN B
      IF (FJCN.NE.0.AND.J.LT.NM) CALL TF((1.,0.)*GAMB(J)/KCBSQ(J)*
&KYB(J),XB,YB,F7,F8)

```

```

0042      GO TO 5C
0043      IF (FJCN .NE. 0 .AND. J .EQ. NM) CALL TF((C.,1.)*OMEGA*MU*1.5*SQRT
      &(3.),XB,YB,FC,FSE)
0044      IF (FJCN .NE. C .AND. J .EQ. NM) CALL TF((1.,0.),XB,XB,FC,FSH)
0045      GO TO 5D
0046      40  DP=KXB(J)*INT1D(F7,F7,F8,F8,XB,XB + BPRM,YB,YB + BCPRM)*KXB(J)
0047      DCP=KYB(J)*INT1D(F5,F5,F6,F6,XB,XB + BPRM,YB,YB + BCPRM)*KYB(J)
0048      B(J)=(C.,1.)*CMEGA/KCBSQ(J)*EPSLGN/KCBSQ(J)*GAMB(J)*(DP + DCP)
0049      AP=KXA(J)*INT1D(F3,F3,F4,F4,XA,XA + APRM,YA,YA + ACPRM)*KXA(J)
0050      ACP=KYA(J)*INT1D(F1,F1,F2,F2,XA,XA + APRM,YA,YA + ACPRM)*KYA(J)
0051      A(J)=(C.,1.)*CMEGA/KCASQ(J)*EPSLGN/KCASQ(J)*GAMA(J)*(AP + ACP)
      C    PRINT 20,CP,DCP
0052      IF (FJCN .NE. 0) CALL TF(GAMB(J)*KXB(J)/KCBSQ(J),XB,YB,F7,F8)
0053      50  CONTINUE
0054      IF (M .LT. NM) GO TO 7C
      C-----READ IN PARAMETERS FOR SPECIAL MODE FORMULATION
0055      REAC 6C,A(10),B(1C)
0056      60  FORMAT (8F10.1)
0057      DUMMY=(C.,1.5)*CMEGA*MU*1.73205
      C-----REPLACE THE NEXT MODE BY SPECIAL MODE
0058      A(10)=A(10)*DUMMY
0059      B(1C)=B(1C)*DUMMY
0060      70  CONTINUE
0061      PRINT 8C,(J,A(J),B(J),J=1,N)
0062      80  FORMAT (//(' AB'12,1X,4G16.8))
      C-----CALCULATE THE CROSS INTEGRAL
0063      DO 14C I=1,M
0064      DO 14C J=1,N
0065      IF (CLASS .EQ. - 1) GO TO 90
0066      XL=XB
0067      XU=XB + BPRM
0068      YL=YB
0069      YU=YB + BCPRM
0070      IF (MODEA(3,I) .EQ. TM) GO TO 12C
0071      IF (MODEB(3,J) .EQ. TM) GO TO 110
0072      GO TO 10C
0073      90  XL=XA
0074      XU=XA + APRM
0075      YL=YA
0076      YU=YA + ACPRM
0077      IF (MODEB(3,J) .EQ. TM) GO TO 12C
0078      IF (MODEA(2,I) .EQ. TM) GO TO 11C
0079      100 GA=GAMA(I)
0080      IF (CLASS .EQ. - 1.) GA=GAMB(J)
0081      CD(I,J)=(C.,1.)*OMEGA/KCASQ(I)*MU/KCBSQ(J)*GA*(KXA(I)*INT1D(F1,F5,
      &F2,F6,XL,XU,YL,YU)*KXB(J) + KYA(I)*INT1D(F3,F7,F4,F8,XL,XL,YL,YU)*
      &KYB(J))
0082      GO TO 140
0083      110 IF (CLASS .EQ. 1.) INT=(( - KXA(I))*INT1D(F1,F5,F2,F6,XL,XU,YL,YU)
      &*KYB(J) + KYA(I)*INT1D(F3,F7,F4,F8,XL,XU,YL,YU)*KXB(J))
0084      IF (CLASS .EQ. - 1.) INT= - (KXA(I)*INT1D(F3,F7,F4,F8,XL,XU,YL,YU)
      &*KYB(J) + KYA(I)*INT1D(F1,F5,F2,F6,XL,XU,YL,YU)*KXB(J))
0085      CD(I,J)=GAMA(I)/KCASC(I)*GAMB(J)/KCBSQ(J)*INT
0086      GO TO 140
0087      120 IF (MODEB(3,J) .EQ. TM .AND. CLASS .EQ. 1.) GO TO 13C
0088      IF (MODEA(3,I) .EQ. TM .AND. CLASS .EQ. - 1) GO TO 13C
0089      IF (CLASS .EQ. 1.) INT=( - KXA(I)*INT1D(F3,F7,F4,F8,XL,XU,YL,YU)*
      &KYB(J) + KYA(I)*INT1D(F1,F5,F2,F6,XL,XL,YL,YU)*KXB(J))
0090      IF (CLASS .EQ. - 1.) INT=(( - KXA(I))*INT1D(F1,F5,F2,F6,XL,XU,YL,
      &YU)*KYB(J) - KYA(I)*INT1D(F3,F7,F4,F8,XL,XU,YL,YU)*KXB(J))

```


0091		CD(I,J)=KSC/(KCASC(I)*KCBSQ(J))*INT	1210
0092		GO TO 14C	1220
0093	130	GA=GAMB(J)	1230
0094		IF (CLASS .EQ. - 1.) GA=GAMA(I)	1240
0095		CD(I,J)=(C.,1.)*CMEGA/KCASQ(I)*EPSLON/KCBSQ(J)*GA*(KXA(I)*INT1C(F3 8,F7,F4,F8,XL,XU,YL,YU)*KXB(J) + KYA(I)*INT1D(F1,F5,F2,F6,XL,XL,YL, &YU)*KYB(J))	1250 1260 127C
0096	140	CONTINUE	1280
0097		IF (M .LT. NM) GO TO 160	1290
	C----	READ IN PARAMETER FOR SPECIAL MODE	1300
0098		READ 60,A10	1310
0099		READ 6C,(CD(I,10),I=1,9),(CD(10,J),J=1,9)	1320
0100		DO 15C I=1,3	1330
	C----	REPLACE NEXT MODE WITH VALUES FOR SPECIAL MODES	1340
0101		CD(I,10)=CD(I,1C)*DUMMY*GAMA(I)/KCASC(I)*KYA(I)	135C
0102	15C	CD(1C,I)=CD(1C,I)*(C., - 1.)*CMEGA*MU/KCBSQ(I)*KYB(I)	1360
0103		CD(10,10)=DUMMY*A10	1370
0104	16C	CONTINUE	1380
0105	17C	FORMAT (//(' CD*2I3,1X,2G16.8))	1390
	C----	CALCULATE SCATTERING MATRIX FOR NEXT JUNCTION TO BE SOLVED	1400
0106		DO 18C I=1,N	1410
0107		DO 180 J=1,N	1420
0108		GL= - SML*(GAMB(I) + GAMB(J))	1430
	C	IF(ABS(GL) .GT. 1.E10) GL=-1.E10	1440
0109	180	S(I,J)=CEXP(GL)*AVEC(J,I)	1450
0110		RETURN	1460
0111		END	1470

0001		SUBROUTINE GAM(MPM,MDPM,XXSYM,YSYM,KSQ,APRM,ADPRM,GAMM,MODE,N)	CC10
0002		REAL KSC,KX,KY	CC20
0003		INTEGER XXSYM,YSYM,YYSYM	CC30
0004		INTEGER*2 TE/'TE'/,TM/'TM'/,MODE(3,30)	CC40
0005		COMPLEX GAMM(30)	CC50
0006		COMPLEX CSQRT,CMLPX	CC60
0007		DATA PI/3.141593/	CC70
0008		YYSYM=YSYM	CC80
0009		IF (YSYM .EQ. C) YYSYM=1	CC90
0010		N=0	C100
0011	10	IF (XXSYM .NE. 0) GC TO 20	C110
0012		MPRM=0	C120
0013		GO TO 30	C130
0014	20	MS=XXSYM	C140
0015		MMPM=MPM + XXSYM	C150
0016		DG 100 MMPM=MS,MMPM,XXSYM	C160
		C-----GENERATES MODES WITH X VARYING	C170
0017		MPRM=MMPM - XXSYM	C180
0018	30	KX=MPRM/AFRM*PI	C190
0019	40	NS=1	C200
0020		DO 80 MDCRMS=NS,MDPM,YYSYM	C210
		C-----GENERATES MODES WITH Y VARYING	C220
0021		MDPRM=MDPRMS	C230
0022		IF (MPRM .EQ. 0 .AND. MDCPRM .EQ. 0) GO TO 80	C240
0023	50	KY=MDPRM/ACPRM*PI	C250
0024		N=N + 1	C260
		C-----CALCULATES PROPGATCIN CONSTANT	C270
0025	60	GAMM(N)=CSQRT(CMPLX(KX*KX + KY*KY - KSC,0.))	C280
		C-----SET UP CODES FOR TE MODE TYPE	C290
0026		MODE(1,N)=MPRM	C300
0027		MODE(2,N)=MDPRM	C310
0028	70	MODE(3,N)=TE	C320
0029		IF (N .GE. 30) GC TO 110	C330
		C-----CHECK FOR POSSIBILITY OF TM MODE TYPE	C340
0030		IF (MPRM .EQ. 0 .OR. MDCPRM .EQ. C) GO TO 80	C350
0031		N=N + 1	C360
		C-----GAMMA IS SAME FOR TM MODE	C370
0032		GAMM(N)=GAMM(N - 1)	C380
0033		MODE(1,N)=MPRM	C390
0034		MODE(2,N)=MDPRM	C400
0035		MODE(3,N)=TM	C410
0036		IF (YSYM .EQ. 2 .AND. MDCPRM .EQ. C) MDCPRM = - 1	C420
0037		IF (N .GE. 30) GC TO 110	C430
0038	80	CONTINUE	C440
		C-----ALL MODE ARE GENERATED IF ONLY TE CN TYPE	C450
0039	90	IF (XXSYM .EQ. 0) GO TO 110	C460
0040	100	CONTINUE	C470
0041	110	CONTINUE	C480
0042		PRINT 120,(MODE(3,I),MODE(1,I),MODE(2,I),GAMM(I),I=1,N)	C490
0043	120	FORMAT (/'(' 'A2,I2,1X,I2,' GAM='2G15.7))	C500
0044		RETURN	C510
0045		END	C520

0001		SUBROUTINE SIMCCM	
0002	C-----	ASSEMBLES INTEGRALS INTO SET OF EQUATIONS	0010
0003		INTEGER R,RMIN,RMAX	0020
0004		REAL LAMBDA	0030
		COMPLEX A(30),AVEC(30,30),B(30),CD(30,30),COEF(31,31),S(30,30),VEC	0040
		&(31),SUM,PRD	0050
0005		COMMON A,B,CD,S,CCEF,VEC,AVEC,M,KAPN,KAPNP1,R,RMIN,RMAX,CLASS	0060
0006		EQUIVALENCE (CLASS,SIGN)	0070
0007		CCEF(1,1)=A(R)	0080
0008		VEC(1)= - SIGN*A(R)	0090
0009		DO 30 J=1,KAPN	0100
0010		SUM=C	0110
0011		DO 10 K=1,KAPN	0120
0012	10	SUM=SUM + CD(R,K)*S(J,K)	0130
0013	20	COEF(1,J + 1)= - SIGN*CD(R,J) - SUM	0140
0014	30	CONTINUE	0150
0015		DO 40 N=1,KAPN	0160
0016		NP1=N + 1	0170
0017		COEF(NP1,1)=CD(R,N)	0180
0018	40	VEC(NP1)=SIGN*CD(R,N)	0190
0019		DO 110 N=1,KAPN	0200
0020		NP1=N + 1	0210
0021		DO 90 J=1,KAPN	0220
0022		SUM=C	0230
0023		DO 80 I=1,M	0240
0024		IF (I .EQ. R) GO TO 80	0250
0025	50	PRD=C.	0260
0026		DO 60 K=1,KAPN	0270
0027	60	PRD=PRD + CD(I,K)*S(J,K)	0280
0028	70	SUM=SUM + CD(I,N)*(SIGN*PRD + CD(I,J))/A(I)	0290
0029	80	CONTINUE	0300
0030	90	COEF(NP1,J + 1)=SIGN*SUM	0310
0031		COEF(NP1,NP1)=SIGN*B(N) + COEF(NP1,NP1)	0320
0032		DO 100 J=1,KAPN	0330
0033		JP1=J + 1	0340
0034	100	COEF(NP1,JP1)=COEF(NP1,JP1) - B(N)*S(J,N)	0350
0035	110	CONTINUE	0360
0036		RETURN	0370
0037		END	0380
			0390

0001		SUBROUTINE SLVEQ(A,B,N,NCIM,C,UNIT)	0010
	C-----	SOLVES A SET OF LINEAR EQUATIONS	0020
0002		INTEGER UNIT	0030
0003		COMPLEX A(NCIM,NCIM),B(N),BIGA,HOLD,D	0040
0004	10	NM1=N - 1	0050
0005		D=1.	0060
0006		DO 80 K=1,NM1	0070
0007		BIGA=A(K,K)	0080
0008		J=K	0090
0009		KP1=K + 1	0100
0010		DO 20 I=KP1,N	0110
0011		IF (CABS(BIGA) .GE. CABS(A(I,K))) GO TO 20	0120
0012		BIGA=A(I,K)	0130
0013		J=I	0140
0014	20	CONTINUE	0150
0015		D=C*BIGA	0160
0016		IF (CABS(D) .EQ. C.) GO TO 100	0170
0017		IF (J .LE. K) GO TO 40	0180
0018		DO 30 I=K,N	0190
0019		HOLD=A(K,I)	0200
0020		A(K,I)=A(J,I)/BIGA	0210
0021	30	A(J,I)=HOLD	0220
0022		HOLD=B(K)	0230
0023		B(K)=B(J)/BIGA	0240
0024		B(J)=HOLD	0250
0025		GO TO 60	0260
0026	40	DO 50 I=KP1,N	0270
0027	50	A(K,I)=A(K,I)/BIGA	0280
0028		B(K)=B(K)/BIGA	0290
0029	60	DO 80 I=KP1,N	0300
0030		DO 70 J=KP1,N	0310
0031	70	A(I,J)=A(I,J) - A(I,K)*A(K,J)	0320
0032	80	B(I)=B(I) - A(I,K)*B(K)	0330
0033		D=D*A(N,N)	0340
0034		IF (CABS(D) .EQ. C.) GO TO 100	0350
0035		B(N)=B(N)/A(N,N)	0360
0036		DO 90 I=1,NM1	0370
0037		K=N - I	0380
0038		KP1=K + 1	0390
0039		DO 90 J=KP1,N	0400
0040	90	B(K)=B(K) - A(K,J)*B(J)	0410
0041		RETURN	0420
0042	100	WRITE (UNIT,110)	0430
0043	110	FORMAT ('SINGULAR SET OF EQUATIONS')	0440
0044		RETURN	0450
0045		END	0460

0001	FUNCTION F1(X)	CC10
	C-----DEFINES FUNCTIONS FOR EACH INTEGRATION	CC20
0002	COMPLEX A(30),B(30),CD(30,30),S(20,30),COEF,GAMB(30),GAMA(30)	CC30
0003	INTEGER*2 MCDEA(3,30)	CC40
0004	REAL KXA(30),KYA(30),KCASQ(30),KXB(30),KYB(30),KCBSQ(30),KSC	CC50
0005	COMMON A,E,CC,S,CCEF,GAMB	CC60
0006	COMMON /MATCCM/GAMA,MCDEA,KXA,KYA,KCASQ,CMEGA,KSQ,XA,YA,XB,YB	CC70
0007	COMMON /FNCTN/I,J	0080
0008	COMMON /GB/KXE,KYB,KCBSQ	CC90
	C-----F1 - F4 FOR A GUIDE	0100
0009	F1=SIN(KXA(I)*(X - XA))	0110
0010	RETURN	0120
0011	ENTRY F2(Y)	0130
0012	F2=COS(KYA(I)*(Y - YA))	0140
0013	RETURN	0150
0014	ENTRY F3(X)	0160
0015	F3=CCS(KXA(I)*(X - XA))	0170
0016	RETURN	0180
0017	ENTRY F4(Y)	0190
0018	F4=SIN(KYA(I)*(Y - YA))	0200
0019	RETURN	0210
0020	ENTRY F5(X)	0220
	C-----F5 - F8 FOR B GUIDE	0230
0021	F5=SIN(KXB(J)*(X - XB))	0240
0022	RETURN	0250
0023	ENTRY F6(Y)	0260
0024	F6=COS(KYB(J)*(Y - YB))	0270
0025	RETURN	0280
0026	ENTRY F7(X)	0290
0027	F7=CCS(KXB(J)*(X - XB))	0300
0028	RETURN	0310
0029	ENTRY F8(Y)	0320
0030	F8=SIN(KYB(J)*(Y - YB))	0330
0031	RETURN	0340
0032	END	0350

0001	SUBROUTINE BASC	0010
C----	CALCULATES BACK SCATTERING COEFFICIENTS	0020
0002	INTEGER R,RMIN,RMAX	0030
0003	REAL LAMBDA	0040
0004	COMPLEX A(30),AVEC(30,30),B(30),CD(30,30),COEF(31,31),S(30,30),VEC	0050
	ε(31),SLM1,SUM2,SLM3	0060
0005	COMMON A,B,CC,S,CCEF,VEC,AVEC,P,λ,NP1,R,RMIN,RMAX,CLASS	0070
C----	SUM IS NEGATIVE FOR ENLARGEMENT	0080
0006	EQUIVALENCE (CLASS,SIGN)	0090
C----	RHO IS FIRST UNKNOWN	0100
0007	AVEC(R,R)=VEC(1)	0110
0008	DO 30 I=1,P	0120
0009	IF (I .EQ. R) GO TO 30	0130
0010	SUM1=0.	0140
0011	DO 20 J=1,N	0150
0012	SUM2=0.	0160
0013	DO 10 K=1,N	0170
0014	10 SUM2=SUM2 + CD(I,K)*S(J,K)	0180
0015	20 SUM1=SUM1 + VEC(J + 1)*(SIGN*SUM2 + CD(I,J))	0190
0016	AVEC(I,R)=SIGN*SUM1/A(I)	0200
0017	30 CONTINUE	0210
0018	RETURN	0220
0019	END	0230

0001	SUBROUTINE TF(CON,R2,R1,FX,FY)	0010
	C-----TOTAL UP FIELD FOR EACH NORMAL WAVEGUIDE MODE	0020
0002	REAL Y(120),DELY/.01/,L(2),U(2),CENTER(2)/1.143,.5/	0030
0003	COMPLEX CCN,FEY(120)	0040
0004	L(1)=R1	0050
0005	L(2)=R2	0060
0006	DO 40 J=1,1	0070
0007	Y(1)=0.	0080
	C-----CALCULATE FIELD IN X AND Y DIRECTIONS	0090
0008	IF (J .EQ. 1) FEY(1)=CON*FX(.5)*FY(Y(1))	0100
0009	IF (J .EQ. 2) FEY(1)=CCN*FX(0.)*FY(1.15)	0110
0010	IF (L(J) .GT. C.) FEY(1)=C.	0120
0011	DO 20 I=2,120	0130
0012	Y(I)=Y(I - 1) + DELY	0140
	C-----CALCULATE FIELD ONLY TO CENTERLINE	0150
0013	IF (Y(I) .GT. CENTER(J)) GO TO 30	0160
	C-----FIELD IS C IF Y IS LESS THAN CRIGIN	0170
0014	IF (Y(I) .GE. L(J)) GO TO 10	0180
0015	FEY(I)=(0.,0.)	0190
0016	GO TO 20	0200
0017	10 IF (J .EQ. 1) FEY(I)=CON*FX(.5)*FY(Y(I))	0210
0018	IF (J .EQ. 2) FEY(I)=CCN*FX(Y(I))*FY(1.15)	0220
0019	20 CONTINUE	0230
0020	30 I=I - 1	0240
	C-----WRITE THE MODE PATTERN TEMPORARILY ON DISK	0250
0021	WRITE (4) I,(FEY(K),K=1,I)	0260
0022	40 CONTINUE	0270
0023	RETURN	0280
0024	END	0290

0001	SUBROUTINE FIELD(VEC,AVEC,M,N)	CC10
CC02	COMPLEX VEC(31),AVEC(30,30),FEY(120),FIELD(120,4)	CC2C
0003	COMMON /BLFF/FEY	0030
CCC4	INTEGER NPTS(4)	CC4C
0005	C-----SIGN IS NEGATIVE FOR H FIELD	CC5C
	REAL SIGN(4)/1.,1., - 1., - 1./	CC6C
	C-----PLACE RECCD AT THE FIRST MCDE	CC7C
0006	REWIND 4	0080
0007	DO 20 J=1,3,2	CC9C
	C-----READ FIRST MCDE FOR E FIELD THEN H FIELD IN A	C100
0008	READ (4) I,(FEY(K),K=1,I)	0110
0009	NPTS(J)=I	C120
	C PRINT 2CC,(FEY(K),K=1,I)	C130
0010	10 FORMAT (' FEY'/(12G11.3))	0140
	C-----CALCULATE FIELD PATTERN DUE TO FIRST MODE	0150
0011	DO 2C K=1,I	C160
0012	20 FIELD(K,J)=(1. + SIGN(J)*AVEC(1,1))*FEY(K)	C170
0013	DO 30 MCDE=2,M	C180
	C-----DUMMY READ TO SKIP FIELD IN GUIDE B	0190
0014	READ (4) I,(FEY(K),K=1,I)	0200
0015	READ (4) I,(FEY(K),K=1,I)	C210
0016	DO 3C J=1,3,2	0220
	C-----READ NEXT E AND F PATTERN FOR GUIDE A	0230
0017	READ (4) I,(FEY(K),K=1,I)	C240
	C PRINT 2CO,(FEY(K),K=1,I)	0250
CC18	DO 30 K=1,I	C260
	C-----ADD THEM TO FIELD	C270
0019	30 FIELD(K,J)=FIELD(K,J) + AVEC(MCDE,1)*FEY(K)*SIGN(J)	C280
CC2C	DO 50 J=1,3,2	C290
0021	I=NPTS(J)	0300
	C-----PRINT OUT TOTAL FIELD PATTERNS FOR GUIDE A	C310
0022	PRINT 4C,(FIELD(K,J),K=1,I)	C320
0023	40 FORMAT ('/' EAX FIELD'/(1X,8G15.7))	0330
	C-----WRITE TOTAL FIELD PATTERNS ON DISK	0340
0024	WRITE (8) I,(FIELD(K,J),K=1,I)	0350
0025	50 CONTINUE	0360
	C-----POSITION TO FIRST RECORD ON DISK AGAIN	0370
0026	REWIND 4	0380
0027	DO 60 K=1,120	C390
CC28	DO 60 J=1,3,2	C400
0029	60 FIELD(K,J)=C.	C410
0030	DO 70 MCDE=2,N	0420
	C-----TWO DUMMY READS TO SKIP FIELDS IN A	C430
0031	READ (4) I,(FEY(K),K=1,I)	0440
0032	READ (4) I,(FEY(K),K=1,I)	C450
0033	DO 7C J=1,3,2	C460
	C-----READ E AND H FIELDS IN GUIDE B	0470
0034	READ (4) I,(FEY(K),K=1,I)	C480
0035	NPTS(J)=I	C490
0036	DO 7C K=1,I	0500
	C-----SUM UP TOTAL FIELD PATTERN IN GUIDE B	C510
0037	70 FIELD(K,J)=FIELD(K,J) + VEC(MCDE)*FEY(K)	C520
0038	DO 80 J=1,3,2	0530
0039	I=NPTS(J)	C540
	C-----WRITE TOTAL FIELD PATTERNS ON DISK	0550
0040	WRITE (8) I,(FIELD(K,J),K=1,I)	0560
	C-----PRINT OUT TOTAL FIELD PATTERN E AND H FIELD GUIDES	C570
0041	80 PRINT 5C,(FIELD(K,J),K=1,I)	0580
0042	90 FORMAT ('/' EBX FIELD'/(1X,8G15.7))	0590
0043	RETURN	0600

CCC1	SUBROUTINE INTEGR(FX,GX,XL,XU,EPS,Y)	CC10
CCC2	LOGICAL TWO	CC20
0003	XC=XU - XL	0030
CCC4	H=XC/100	CC40
0005	N=XC/H + .5	CC50
0006	N=N/2*2	CC60
CCC7	H=XC/N	CC70
CCC8	NM1=N - 1	CC80
0009	SUM=0	CC90
CC10	TWO= .FALSE.	C100
0011	DO 10 I=1,NM1	C110
0012	X=I*H + XL	C120
CC13	MULT=4	C130
0014	IF (TWO) MULT=2	0140
0015	TWO= .NOT. TWO	C150
CC16	10 SUM=SUM + MULT*FX(X)*GX(X)	0160
0017	SIMP=(SUM + FX(XU)*GX(XU) + FX(XL)*GX(XL))*H/3	0170
0018	Y=SIMP	0180
CC19	RETURN	C190
0020	END	0200

A.2 Modal Equation Derivation

This derivation is given by Wexler (1) and is repeated here with a slight generalization for the incident mode.

Assuming an orthogonal set of modes in each guide section described in (2.1) to (2.4), then for $i \neq m$

$$\int_a \bar{e}_{ai} \times \bar{h}_{am} \cdot \tilde{u}_z \, ds = 0 \quad (\text{A.2.1})$$

Equate (2.1) and (2.3) and take the cross product of each term with \bar{h}_{am} and integrate over the cross section of $A^{(m)}$. For simplicity of notation let

$$\alpha_i = \int_a \bar{e}_{ai} \times \bar{h}_{ai} \cdot \tilde{u}_z \, ds \quad (\text{A.2.2})$$

and

$$\delta_{ji} = \int_b \bar{e}_{bj} \times \bar{h}_{ai} \cdot \tilde{u}_z \, ds \quad (\text{A.2.3})$$

we then have

$$(1 + \rho_r) a_r \alpha_r = \sum_{j=1}^{\infty} b_j (\delta_{jr} + \sum_{k=1}^{\infty} s_{jk} \delta_{kn}) \quad m = r \quad (\text{A.2.4})$$

and

$$a_i \alpha_i = \sum_{j=1}^{\infty} b_j (\delta_{ji} + \sum_{k=1}^{\infty} s_{jk} \delta_{ki}) \quad m \neq r \quad (\text{A.2.5})$$

Equate (2.2) and (2.4) and take the cross product of each term with \bar{e}_{bn} and integrate over the cross section of guide $B^{(m)}$.

Using the orthogonality condition

$$\int_b \bar{e}_{bn} \times \bar{h}_{bj} \cdot \tilde{u}_z \, ds \quad (\text{A.2.6})$$

and the notation

$$\beta_j = \int_b \bar{e}_{bj} \times \bar{h}_{bj} \cdot \tilde{u}_z \, ds$$

we have

$$(1 - \rho_r) a_r \delta_{nr} - \sum_{\substack{i=1 \\ i \neq r}}^{\infty} a_i \delta_{ni} = (b_n - \sum_{j=1}^{\infty} b_j s_{jn}) \beta_n \quad (\text{A.2.7})$$

using continuity of the magnetic field.

Substituting (A.2.5) into (A.2.7) and re-arranging we get

$$\rho_r \delta_{nr} + \sum_{j=1}^N \frac{b_j}{a_r} \sum_{\substack{i=1 \\ i \neq r}}^M \frac{\delta_{ji} + \sum_{k=1}^N s_{jk} \delta_{ki} \delta_{ni}}{\alpha_i} \quad (\text{A.2.8})$$

and from (A.2.4) we get

$$\rho_r \alpha_r - \sum_{j=1}^N \frac{b_j}{a_r} (\delta_{jr} + \sum_{k=1}^N s_{jk} \delta_{kr}) = -\alpha_r \quad (\text{A.2.9})$$

The equations were truncated at M and N modes in waveguides A⁽¹⁾ and B respectively. The boundary enlargement problem results in similar equations but some integrations are over different limits and there are some sign changes. For completeness the general equations are given in (2.5) to (2.12).

Equation (A.2.5) can be re-written to give $\frac{a_i}{a_r}$ and is given in (2.13).

BIBLIOGRAPHY

- (1) A. Wexler, "Solution of Waveguide Discontinuities by Modal Analysis," IEEE Trans. on Microwave Theory and Techniques, Vol. MTT-15, September 1967, pp. 508-517.
- (2) P. J. B. Clarricoats and K. R. Slinn, "Numerical Method for the Solution of Waveguide Discontinuity Problems," Proc. IEE., 1967, 114, pp. 878-886.
- (3) W. J. Cole, E. R. Nagelberg and C. M. Nagel, "Iterative Solution of Waveguide Discontinuity Problems," Bell Syst. Tech. J., 1967, 46, pp. 649-722.
- (4) A. Wexler, (1) pp. 509-511.
- (5) N. Marcuvitz, Waveguide Handbook. New York: McGraw-Hill, 1951, pp. 168-172.
- (6) A. Wexler, (1) p. 513
- (7) N. Marcuvitz, (5) pp. 168-170
- (8) Ibid. p. 296.
- (9) Ibid. p. 296
- (10) Ibid. p. 407.
- (11) Ibid. pp. 406-407.
- (12) A. Wexler, (1) p. 514.
- (13) N. Marcuvitz, (5) p. 255.
- (14) Ibid. pp. 221-224.
- (15) P. H. Masterman, P. J. B. Clarricoats and C. D. Hannaford, "Waveguide Iris Problems," Electronics Letters, 1969, Vol. 5, No. 2, pp. 23-25.
- (16) N. Marcuvitz, (5), pp. 307-309.
- (17) Ibid. pp. 404-406.
- (18) Ibid. pp. 218-220.
- (19) J.W. Bandler, "Computer Optimization of Inhomogeneous Waveguide Transformers," IEEE Trans. on Microwave

Theory and Techniques, Vol. MTT-17, August 1969, pp. 564-566.

- (20) R. M. Walker, Microwave Transmission Lines. New York: McGraw-Hill, 1948, pp. 220-222.
- (21) J. Van Bladel, Electromagnetic Fields. New York: McGraw-Hill, 1964, p. 387.
- (22) L. Fox and A. Sankar, "Boundary Singularities in Linear Elliptic Differential Equations," Journal of Institute of Mathematical Applications, 1969, 5, pp. 340-350.
- (23) C.-E. Froberg, Introduction to Numerical Analysis. Reading, Mass.: Addison-Wesley, 1965, pp. 172-173.
- (24) A. Wexler, (1) pp. 512-515.
- (25) N. Marcuvitz, (5) pp. 172-174.
- (26) J. Van Bladel, (21) pp. 385-386.
- (27) A. Wexler, (1) pp. 512-513.
- (28) A. Wexler, (1) p. 513.